DEPARTMENT OF CHEMISTRY, UNIVERSITY OF JYVÄSKYLÄ RESEARCH REPORT No. 162

THEORETICAL AND EXPERIMENTAL STUDIES OF SOME MAIN GROUP COMPOUNDS: FROM CLOSED SHELL INTERACTIONS TO SINGLET DIRADICALS AND STABLE RADICALS

BY

JANI MOILANEN

Academic Dissertation for the Degree of
Doctor of Philosophy

To be presented,
by permission of the Faculty of Mathematics and Science of the University of Jyväskylä,
for public examination in KEM4, on December 13th, 2012 at 12 noon.

UNIVERSITY OF JYVÄSKYLÄ

Jyväskylä, Finland
ISBN 978-951-39-4962-4
ISSN 0357-346X

ABSTRACT

Moilanen, Jani
Theoretical and Experimental Studies of Some Main Group Compounds: From Closed Shell Interactions to Singlet Diradicals and Stable Radicals
Jyväskylä: University of Jyväskylä, 2012, p. 80
(Department of Chemistry, University of Jyväskylä Research Report
ISSN 0357-346X)
ISBN 978-951-39-4962-4

Acquiring knowledge of different interactions within and between molecules is a fascinating undertaking as it not only deepens our understanding of chemical bonding but also offers insight into electronic structures, molecular properties and the connections between these two. This dissertation combines together three main group chemistry related topics within the aforementioned theme.

Research presented in the first third of this dissertation describes wave function and density functional theory studies of weak inter- and intramolecular interactions in pnictogen-based dimers $X_3Pn\cdots PnX_3$ (Pn = N-Bi; X = F-I), dithallenes RTlTlR (R = H, Me, ^{t}Bu, Ph) and octachalcogen dications Ch_8^{2+} (Ch = S, Se). The conducted theoretical work revealed that dynamic electron correlation effects play a key role in the bonding of all examined systems. Most importantly, the results showed that the investigated Pn···Pn interactions are sufficiently strong to be useful in crystal engineering and they also provided the first comprehensive picture of transannular bonding in Ch_8^{2+}.

The second third of this dissertation focuses on the analysis of bonding interactions in group 13 dimetallenes REER (E = Al-In; R = H, Me, ^{t}Bu, Ph) and in tetrachalcogen tetranitrides Ch_4N_4 (Ch = S, Se). The use of highly accurate theoretical methods provided insight into bonding in these systems and demonstrated that their electronic structures contain an important multiconfigurational component which had not been recognized before. Consequently, the published results give valuable new information about diradical contributions to bonding and serve as an illustrative example of the important role computational and theoretical methods nowadays play in the characterization of molecular systems.

The last third of this dissertation discusses the results from systematic computational and experimental efforts targeting new stable radicals based on the ubiquitous β-diketiminate ligand. Density functional theory calculations, together with the characterization of the first spirocyclic aluminum bis-β-diketiminate radical, proved that this ligand framework offers a potential building block for the synthesis of a wide variety of new paramagnetic metal-ligand architectures.

Keywords: main group chemistry, theoretical and computational chemistry, synthesis, intermolecular interactions, intramolecular interactions, stable radicals, singlet diradical character, closed shell interactions

Author's address

Jani Moilanen
Department of Chemistry
P.O. Box 35
FI-40014 University of Jyväskylä
Finland
jani.o.moilanen@jyu.fi

Supervisors

Adjunct Professor Heikki M. Tuononen
Department of Chemistry
University of Jyväskylä
Jyväskylä, Finland

Associate Professor Roland Roesler
Department of Chemistry
University of Calgary
Calgary, Canada

Professor Jussi Valkonen
Department of Chemistry
University of Jyväskylä
Jyväskylä, Finland

Reviewers

Professor Markku Räsänen
Department of Chemistry
University of Helsinki
Helsinki, Finland

Professor Risto Laitinen
Department of Chemistry
University of Oulu
Oulu, Finland

Opponent

Professor Tapani Pakkanen
Department of Chemistry
University of Eastern Finland
Joensuu, Finland

PREFACE

The work presented in this dissertation was carried out at the Departments of Chemistry in Universities of Jyväskylä, Calgary and Lethbridge between the summer 2008 and autumn 2012.

I wish to express my deepest gratitude to my supervisors Adjunct Prof. Heikki M. Tuononen, Associate Prof. Roland Roesler and Prof. Jussi Valkonen for their guidance, criticism and encouragement throughout the work. In particular, I would like to thank my primary supervisor Adjunct Prof. Tuononen for giving me the opportunity to join his group and undertake the research project. It has been a great pleasure for me to work with such a talented researcher. In addition, I am especially thankful to Associate Prof. Roland Roesler who supervised me during the experimental part of this research project at the University of Calgary. My warmest thanks also go to Prof. René Boeré and Dr. Tracey Roemmele for introducing me to the fine art of EPR spectroscopy and electrochemistry.

The reviewers of this dissertation, Prof. Markku Räsänen and Prof. Risto Laitinen, are warmly acknowledged for their valuable comments and suggestions. Prof. Emer. Tristram Chivers is thanked for proofreading this work.

I would also like to express my sincerest thanks to all co-workers from the groups of Prof. Tuononen, Roesler and Boeré. I am particularly indebted for M.Sc. Anssi Peuronen, M.Sc. Mikko Hänninen, B.Sc. Javier Borau-Garcia and Dr. Matthew Hobbs who not only shared office space with me but also many of the scientific and daily life discussions. I also wish to thank the technical and administration staff from the Universities of Jyväskylä, Calgary and Lethbridge, as well as all other people that have helped me during the past years.

Even though I have had great opportunity to work in inspiring research environments with wonderful co-workers, this work would not have been completed without the support of my parents, sister and friends. Thank you all for being part of my life and bringing both strength and happiness to my days.

Most of all, I am more than grateful to my wife Sanna who has shared the ups and downs with me during these four years I have been working towards my dissertation. Thank you for your love, warmth and support!

The financial support from the University of Jyväskylä, the Academy of Finland, the Inorganic Materials Chemistry Graduate Program (EMTKO), the Technology Industries of Finland Centennial Foundation, the Magnus Ehrnrooth Foundation and the Ellen and Artturi Nyyssönen Foundation is gratefully acknowledged. My warm thanks also go to CSC - the IT Centre for Science Ltd for the computing resources they have provided to the individual projects.

Jyväskylä 6.11.2012

Jani Moilanen

LIST OF ORIGINAL PUBLICATIONS

This dissertation is based on the following original research papers which are herein referred to by their Roman numerals.

I Moilanen Jani, Ganesamoorthy Chelladurai, Balakrishna Maravanji S. and Tuononen Heikki M., **Weak Interactions between Trivalent Pnictogen Centers: Computational Analysis of Bonding in Dimers $X_3E\cdots EX_3$ (E = Pnictogen, X = Halogen)**, *Inorg. Chem.* **2009**, *48*, 6740-6747.

II Moilanen Jani, Karttunen Antti J., Tuononen Heikki M. and Chivers Tristram, **The Nature of Transannular Interactions in E_4N_4 and E_8^{2+} (E = S, Se)**, *J. Chem. Theory Comput.* **2012**, *8*, 4249-4258.

III Moilanen Jani, Power Philip P. and Tuononen Heikki M., **Nature of Bonding in Group 13 Dimetallenes: a Delicate Balance between Singlet Diradical Character and Closed Shell Interactions**, *Inorg. Chem.* **2010**, *49*, 10992-11000.

IV Moilanen Jani, Borau-Garcia Javier, Roesler Roland and Tuononen Heikki M., **Paramagnetic Aluminium β-Diketiminate**, *Chem. Commun.* **2012**, *48*, 8949-8951.

Author's contribution

The author of the present dissertation has performed all quantum chemical calculations reported in the original research Papers **I-IV**. With regards to experimental work, the author of the present dissertation has done all synthetic preparations and characterizations reported in the original research Paper **IV** except for two X-ray crystal structure analyses. The author has written the first manuscript drafts for research Papers **I-IV**.

Other contributions

List of author's other publications that are related to the topic but not included in this dissertation.

i Caputo Christine A., Koivistoinen Juha, Moilanen Jani, Boynton Jessica N., Tuononen Heikki M. and Power Philip P., **The Mechanism of the Addition of Simple Olefins and Hydrogen to a Heavy Group 13 Alkene Analogue**, *manuscript in preparation*.

CONTENTS

ABBREVIATIONS

AIM	atoms in molecules
ALL	Andersson-Langreth-Lundqvist density functional
AO	atomic orbital
B3LYP	Becke's three parameter hybrid exchange functional with Lee, Yang and Parr correlation functional
BLYP	Becke's exchange functional with Lee, Yang and Parr correlation functional
BSSE	basis set superposition error
BSIE	basis set incompleteness error
CAS	complete active space
CASPT2	complete active space with dynamic electron correlation via second order Møller-Plesset perturbation theory
CBS	complete basis set limit
CC	coupled cluster
CC2	approximate coupled cluster with single and double excitations
CCSD	coupled cluster with single and double excitations
CCSD(T)	coupled cluster with single and double excitations and perturbative treatment of triple excitations
CI	configuration interaction
CISD	configuration interaction with single and double excitations
CIS(D)	configuration interaction with single excitations and perturbative treatment of double excitations
CISD(T)	configuration interaction with single and double excitations and perturbative treatment of triple excitations
CP	counterpoise method
CP-MP2	counterpoise corrected second order Møller-Plesset perturbation theory
DFT	density functional theory
DFT-D	density functional theory with semi-empirical dispersion correction
DNA	deoxyribonucleic acid
EPR	electron paramagnetic resonance
FCI	full configuration interaction
gCP	geometrical counterpoise
HF	Hartree-Fock
HOMO	highest occupied molecular orbital
LCCSD(T)	local coupled cluster with single and double excitations and perturbative treatment of triple excitations
LCM	local correlation method
LMP2	local second order Møller-Plesset perturbation theory
LMO	localized molecular orbitals

LUMO	lowest unoccupied molecular orbital
M06-2X	the 2006 version of Truhlar's hybrid meta exchange-correlation functional with double the amount of nonlocal exchange
M06-HF	the 2006 version of Truhlar's hybrid meta exchange-correlation functional with the full Hartree-Fock amount of nonlocal exchange
M05-2X	the 2005 version of Truhlar's hybrid meta exchange-correlation functional with double the amount of nonlocal exchange
MCSCF	multiconfigurational self-consistent field
MM	molecular mechanics
MO	molecular orbital
MP2	second order Møller-Plesset perturbation theory
MP3	third order Møller-Plesset perturbation theory
MP4	fourth order Møller-Plesset perturbation theory
MPPT	Møller-Plesset pertubation theory
MPW91MPW91	modified Perdew-Wang exchange-correlation functional
MRCI	multireference configuration interaction
MRCI+Q	multireference configuration interaction with correction for quadruple excitations
MRCI+QP	multireference configuration interaction with Pople correction for quadruple excitations
NMR	nuclear magnetic resonance
NO	natural orbital
NOON	natural orbital occupation number
PAO	projected atomic orbital
PBE0	Adamo's and Barone's hybrid version of exchange-correlation functional by Perdew, Burke and Ernzerhof
PBE0-D	Adamo's and Barone's hybrid version of exchange-correlation functional by Perdew, Burke and Ernzerhof with semi-empirical dispersion correction
PBE	exchange-correlation functional by Perdew, Burke and Ernzerhof
PBE-D	exchange-correlation functional by Perdew, Burke and Ernzerhof with semi-empirical dispersion correction
PTM	polychlorinated triphenylmethyl radical
QCISD	quadratic configuration interaction with single and double excitations
QCISD(T)	quadratic configuration interaction with single and double excitations and perturbative treatment of triple excitations
QM	quantum mechanics
RAS	restricted active space
RHF	restricted Hartree-Fock
SAPT	symmetry adapted perturbation theory

SCF	self-consistent field
SCS	spin component scaling
SCS-CCSD	spin component scaled coupled cluster with single and double excitations
SOMO	singly occupied molecular orbital
SOS-MP2	scaled opposite spin second order Møller-Plesset perturbation theory
THF	tetrahydrofuran
TPSSTPSS	exchange-correlation functional of Tao, Perdew, Staroverov and Scuseria
UHF	unrestricted Hartree-Fock
vdW-DF	van der Waals density functional
X3LYP	extended hybrid exchangefunctional combined with Lee-Yang-Parr correlation functional

1 INTRODUCTION

By definition, molecules consist of two or more atoms that are held together by strong bonding interactions.[1] In contrast, it is interactions of a much weaker nature that typically act between molecules and are the most ubiquitous forces functioning at the nanoscale.[2,3] In general, the stronger the interaction between two atoms, the closer they are to each other.[4] Thus, interatomic distance is usually held as a good indicator of whether different interactions originate from strong covalent bonding or result from other weaker forces. However, sometimes it is difficult to assign the nature of a specific bonding interaction solely based on the observed interatomic distance. This holds, for example, for many bonding situations between group 13 elements.[5,6,7,8,9] In such a case, sophisticated quantum chemical methods are needed to unambiguously determine the physical origin of the observed interaction or the total lack of it. The detailed investigation of bonding interactions is also important because even small changes in how molecules interact can alter the solid state structures of compounds, which, in turn, can have a drastic effect to the properties of the bulk material such as its conductance and magnetism.[10] If these structure-property relationships could be identified and understood already at the molecular level, it would greatly help in the rational design of new molecule-based materials.

This dissertation has been divided into three main parts, each consisting of separate sections devoted to theory as well as to results and discussion. The individual theory sections are not comprehensive reviews of their topics but only introduce the most relevant material related to the subsequent discussion. In a similar manner, the results and discussion sections only highlight the main outcomes of the computational and experimental work which has been conducted during this research project. The first part of the dissertation focuses on intra- and intermolecular interactions, and the aim of this study was to characterize the physical origin of different bonding interactions between and within main group element species. The aim of the second part of the dissertation was to investigate the complex electronic structures of group 13 dimetallenes and tetrachalcogen tetranitrides through sophisticated multiconfigurational methods capable of describing diradical contributions to bonding. The third part of the

dissertation concentrates on experimental and computational studies on the β-diketiminate ligand and its spirocyclic group 13 complexes. The target of this study was to use the β-diketiminate molecular framework in building new stable neutral spiroconjugated radicals.

2 WEAK INTRA- AND INTERMOLECULAR INTERACTIONS IN MAIN GROUP SYSTEMS

In the absence of strong electrostatic or covalent interactions, intermolecular forces, especially van der Waals forces, become predominant and sometimes they are the only forces acting between molecular assemblies or atoms, such as in noble gas dimers.[2,3] Hence, van der Waals forces influence the physical properties of matter like its melting point, boiling point, vapor pressure, viscosity, surface tension and solubility.[2] Van der Waals forces can also act in an intramolecular fashion and they often fix the structures of larger molecules into specific conformations. Consequently, van der Waals forces play a crucial role in many chemical phenomena such as catalysis[11] and thermochemistry of organic reactions,[12] whereas in biological systems they determine the secondary, tertiary and quaternary structures of proteins and enzymes, and are responsible for the stacking of base pairs in DNA.[2,3] Thus, van der Waals forces have a vital impact on life as we know it.

The standard definition of van der Waals forces includes three different interactions: the dipole-dipole, dipole-induced dipole and London forces a.k.a dispersion forces.[13] The dipole-dipole force can be either attractive or repulsive, depending on the relative orientation of the permanent dipoles, while the dipole-induced dipole and dispersion force are always attractive.[2] The dipole-dipole and dipole-induced dipole forces are usually stronger than dispersion since they arise from the interaction between two molecules of which either both (in case of the dipole-dipole interaction) or only one (in case of dipole-induced dipole interaction) has a permanent electric dipole moment. Contrary to this, the dispersion force originates from transient multipoles that all molecules possess,[i] making it a weak but omnipresent interaction between all molecules, even those that are nonpolar.

Archetypical examples of closed shell interactions dominated by the dispersion force are π···π[14] and CH···π[15] interactions that are mainly found in or-

[i] Transient multipoles stem from the fact that the electron density is distributed unevenly in space due to the non-static nature of any electronic distribution.

ganic molecules. A plethora of molecular systems are also known in which closed shell interactions take place between main group atoms,[16,17] heavy metals[18,19] or even between main group atoms and heavy metals.[20] An exceptionally strong manifestation of the dispersion force is the aurophilic interaction between Au(I) centers.[18] This interaction is further strengthened by relativistic effects and its energy varies from 30 to 50 kJ mol^{-1} as measured by temperature dependent nuclear magnetic resonance (NMR). Similar interactions between other closed shell (d^{10} or $d^{10}s^2$) metal ions, albeit much weaker, have also been reported.[19] Thus, these attractive forces can be called more generally metallophilic interactions. Even though the metallophilic interaction constitutes a relatively new design element in supramolecular chemistry, it has received intense interest as a building block for multidimensional functional materials[21] since it is capable of organizing molecules into dimers, oligomers and infinite chains, as well as two-dimensional sheets.[18,19]

In recent years, molecules containing main group atoms, in particular chalcogens (Ch), have received wide interest in the field of supramolecular chemistry since they can form nanotubes[16f] and molecular systems that have columnar architectures held together primarily by dispersion.[16e] This is rather spectacular because the dispersion force does not show much directionality and, owing to this, usually network-like structures are obtained. In addition to the Ch···Ch interaction,[16] the ability of pnictrogen (Pn) elements to participate in Pn··π interactions has recently been used as a specific design element in supramolecular systems[22] and there are also reports of many other weak interactions involving main group atoms in the literature.[17,20] However, a deeper theoretical understanding of these interactions, like that of the metallophilic interaction, is in many cases lacking. This severely hinders their use as building blocks in structural chemistry. Moreover, if the non-directional nature of the dispersion force could be fixed, for example by modifying the chemical environment (sterics) around main group atoms,[16f,e] it could offer an effective and versatile tool for the rational design of new supramolecular and self-assembled systems containing main group elements.

Due to the physical origin of the dispersion force, not all quantum chemical methods are capable of describing it. Thus, in the following two subchapters, the abilities and inabilities of different theoretical methods to describe dispersion are first discussed and then the specific case studies reported in detail in research Papers **I-III** are reviewed. Specifically, the original research Paper **I** discusses weak intermolecular pnictogen···pnictogen interactions and their quantification with computational methods. In the original research Paper **II**, weak intramolecular interactions in polyatomic cationic chalcogen rings are examined using high-level approaches, whereas in the research Paper **III**, a theoretical description of the nature of bonding in dithallenes is given.

2.1 Quantum chemical methods for the calculation of dispersion force

2.1.1 *Ab initio* methods

The simplest approximation of a multi-electron wave function in *ab initio* electronic structure theory is the Hartree-Fock (HF) model.[23] In this model, the electronic wave function of a system having N electrons is described with a single Slater determinant that consists of N spin orbitals. The approximation ensures that the wave function is antisymmetrized and does not violate the Pauli exclusion principle,[ii] but unfortunately it does not take into account either dynamic or static electron correlation effects. It is a well-known fact that dynamic correlation effects are particularly important for the description of closed shell interactions from which the dispersion force originates. However, the HF model comprises a convenient starting point for other more accurate approximations such as Møller-Plesset perturbation theory (MPPT),[24] configuration interaction (CI)[25,26b] and coupled cluster (CC),[26] which are all suitable quantum chemical methods for modeling a large variety of inter- and intramolecular interactions.

The second order Møller-Plesset perturbation theory (MP2) has been a very successful approach to include dynamic electron correlation effects into the wave function.[23] It offers reasonable accuracy with low computational cost and gives size-consistent correlation energies. Size-consistency means that the energy of a supermolecule AB equals the sum of individual energies of A and B (if A and B are two non-interacting molecules), and it is of particular importance when calculating the interaction energies of weakly bound systems. Despite the popularity of the MP2 method in describing correlation effects, it is not the best method to be used for modeling weak interactions such as the dispersion force since it usually overestimates binding in weakly bound systems. Therefore it gives only a semi-quantitative picture of bonding.[27] This drawback can, however, be fixed, at least to some extent, by using spin component scaling[28] or removing basis set superposition error[29] with either counterpoise correction[30] or by using local correlation methods.[31,iii] The MP3 and MP4 methods that expand the perturbation up to the third and fourth order, respectively, can also be used to improve MP2 results, but they represent less successful compromises between computational cost and accuracy than MP2.[23] In addition, the MPPT series does not converge unconditionally in every case.[23] Thus, for ob-

[ii] The Pauli exclusion principle says that two identical electrons (more generally, two identical fermions) cannot occupy the same quantum state simultaneously. This means that the electronic wave function must be antisymmetric (change sign) upon exchange of two electrons.

[iii] Basis set superposition error is also a problem with other correlated *ab initio* methods, whereas it is typically negligible within density functional theory. Basis set superposition error, spin component scaling and local correlation methods are discussed in more detail in Sections 2.1.3-2.1.5.

taining quantitative accuracy of intermolecular interactions, CC or CI methods should be used.[27]

The CI method can be used to model chemical systems which contain a varying amount of electron correlation and it will give the exact (non-relativistic) energy for a given basis set if the full-CI (FCI) approach is used.[23,25,26b] Thus, on purely theoretical grounds, it is also the method of choice for modeling weak interactions. However, the CI wave function is constructed as a linear combination of excited Slater determinants, weighted by expansion coefficients. Owing to this, as the size of the system increases, the amount of configurations needed to recover the full electron correlation energy increases so rapidly that the FCI wave function can only be used for the smallest of systems. To lower the computational cost of the CI method, the wave function can be truncated to any excitation level. One of the most widely used CI methods is CISD that includes all single and double excitations from the HF reference function. Unfortunately, the CISD method, like all other truncated CI methods, is not size-consistent and is therefore not applicable for modeling weak interactions. This problem can be fixed by introducing quadruple terms into configuration coefficients which approximate the contributions from higher order excitations to the wave function.[32] The model can further be improved if an approximate treatment of triple excitations is included via perturbation theory, yielding the very effective and accurate QCISD(T) approach. The QCISD(T) method is especially tailored for calculating chemical systems whose wave functions are dominated by strong dynamic electron correlation effects.[23,25,26b]

Electron correlation effects can also be taken into account with the CC model that overcomes the size-consistency problem of truncated CI methods simply by construction.[23,33] That is, in the CC approach, all excitations are written in terms of exponential cluster operators, which ensures that the nonlinear terms, generated as products of lower level cluster operators, are also included in the truncated wave function. For example, the CCSD method contains contributions from triple and higher excitations that are products of single and double excitations. Owing to this, the truncated CC methods maintain size-consistency and recover more electron correlation than the corresponding truncated CI methods, all within the same computational cost. Therefore, the use of any other truncated CI method than QCISD(T) cannot really be justified. A particularly powerful CC method is CCSD(T) that has been proven to give very accurate energies and properties for systems whose electronic structures are dominated by a single Slater determinant. However, the CCSD(T) method is to some extent also able to describe near degeneracy effects and it can therefore be used to model systems with a small amount of static electron correlation in their wave function.[iv] The only real disadvantage of the CCSD(T), and the analogous QCISD(T), method is that they can be readily applied to only small or medium sized molecular systems, due to their high computational cost. This means that, in many cases, model systems must be used in the calculations in place of real

[iv] For a more detailed discussion about multiconfigurational methods and static electron correlation, see Chapter 3.

molecules. Alternatively, a part of the molecule can be treated at a lower level of theory, as in QM/MM and QM/QM methods, or the geometry of the molecule can be optimized using a computationally less intensive approach and only energies and molecular properties are calculated at a higher level of theory.

2.1.2 Density functional theory

Density functional theory (DFT) provides an alternative and highly efficient approach to calculate the electronic energies and properties of chemical systems since it utilizes the electron density in place of a wave function.[34] The reduction in computational cost arises from the fact that the electron density depends only on three spatial coordinates, whereas the electronic wave function naturally depends on the coordinates of all electrons and becomes more complex as the number of electrons grows. In principle, DFT gives the exact (non-relativistic) electronic energy of the system of interest if the universal functional linking electron density to energy is known, as shown by the two famous Hohenberg-Kohn theorems.[35] Unfortunately, the exact form of the linking functional is not known and, because of this, approximations need to be employed.[34,36] Consequently, the majority of calculations within the DFT framework of electronic structure theory are currently carried out employing the Kohn-Sham formalism that utilizes a reference determinant (similar to a wave function) to make the problem computationally tractable.[36] At the same time, all terms that cannot be calculated exactly are combined in an exchange-correlation functional which forms the big unknown in DFT. Another caveat is the increase in computational cost of the method which is now similar to traditional HF.

Intensive development on exchange-correlation functionals has gradually led to the situation that modern DFT can recover a substantial amount of electron correlation energy and therefore describe many chemical phenomena, including some non-covalent interactions, with accuracy comparable to the MPPT and CC methods.[37] However, due to the local nature of many exchange-correlation functionals, they are not able to describe the dispersion force which is a purely nonlocal phenomenon and originates solely from long-range electron correlation.[2,34] Various computational approaches have been suggested to overcome this deficiency since the DFT formalism is otherwise well-suited for accurate calculations of large chemical systems that cannot be treated with wave function-based methods.[38,39,40,41,42,43,44,45]

The most popular method to correct the dispersion problem in DFT is the DFT-D ansatz.[v,39] In this approach, the dispersion energy is included as an add-on term to the standard energy given by Kohn-Sham DFT,

$$E_{DFT-D} = E_{KS-DFT} + E_{disp}, \tag{2.1}$$

[v] Searching Web of Knowledge for the three papers describing the original and two modified versions of DFT-D shows that they are currently (as of November 6, 2012) cited a total of 3215 times.

where $E_{KS\text{-}DFT}$ is the Kohn-Sham energy obtained using the standard exchange correlation functional and E_{disp} is the dispersion correction to energy.[39] The first (DFT-D1)[39a] and second (DFT-D2)[39b] versions of this method were purely empirical and, thus, applicable to a limited number of elements and parameterized only for specific functionals. However, the third modification of the method (DFT-D3)[39c] can be used for all elements in the periodic table and coupled to any standard density functional. This stems from the fact that, in DFT-D3, the most important parameters (pairwise specific atomic dispersion coefficients and cutoff radii)[vi] are calculated from first principles. This also improves the accuracy of the approach and DFT-D3 is usually within 10 % of the results obtained with CCSD(T).

Other methods similar to the DFT-D3 approach (developed from first principles) have also been proposed but not widely employed.[40,41,42] The dispersion problem in DFT can, however, be addressed with other methods that have vastly different theoretical backgrounds compared to DFT-D. These include range-separated hybrid methods treating long-range electron correlation with MP2 or CCSD(T),[43] specially designed explicitly nonlocal functionals such as the Andersson-Langreth-Lundqvist (ALL)[44b] and van der Waals density functionals (vdW-DF),[44a] and the symmetry adapted perturbation theory (DFT-SAPT) formalism.[38] Furthermore, some correction for dispersion can be included in DFT through parameterization of the functional by including van der Waals complexes in the employed fitting set.[45] Examples of density functionals using this design principle include M06-2X,[45b] M05-2X[45c] and X3LYP.[45d]

2.1.3 Spin component scaling

Spin component scaling (SCS) is a simple and significant improvement to the traditional MP2 method.[28, 46] In this correction scheme, the same spin and opposite spin components of the second order correlation energy are scaled to fit reaction energy data obtained at the QCISD(T) level of theory.[28c] Thus, SCS is an empirical *ad hoc* correction to the calculated MP2 energies, but it performs much better than the parent MP2 method without any additional computational cost and yields molecular structures, vibrational frequencies and thermodynamic properties in good agreement with experimental data.[28] Furthermore, the SCS-MP2 method can be used to improve the description of weak interactions by using scaling parameters specially tailored for systems with non-covalent interactions.[47]

Because the SCS scheme is an empirical *ad hoc* correction to the correlation energy, it can also be combined with other *ab inito* methods than MP2.[46,48,49,50] Particular interest has been given to coupled cluster-based methods, such as SCS-CCSD, since they typically outperform all MP2-type methods in description of weak interactions.[48] For example, the SCS-CCSD method gives interac-

[vi] The atomic pairwise dispersion coefficient takes into account the polarizabilities of two atoms, whereas the cutoff radii determine the interatomic distance region in which the dispersion energy decreases and eventually vanishes.

tion energies for benzene and methane dimers which are in almost perfect agreement with the CCSD(T) data.[48b] Another CC method for which the SCS scheme is implemented is the approximate coupled cluster singles and doubles (CC2)[51] and it has been proved that this method systematically improves excitation energies of organic molecules when compared to the parent approach.[49] In addition to CC methods, the SCS formalism can also be used to ameliorate the CIS(D) method in which the double excitations are included into the CI wave function via perturbation theory.[50] As observed for CC2, also SCS-CIS(D) approach gives better excitation energies than CIS(D).

Although the SCS formalism is a powerful tool to improve *ab initio* methods, it should be noted that it is not itself strictly *ab initio*,[28c] and also not the only approach that takes advantage of spin component scaling parameters. Other similar approaches have been developed, such as the scaled opposite spin second order perturbation theory method (SOS-MP2), in which only the component of opposite spins is parameterized towards a specific training set.[52] The performance of the SOS-MP2 approach is rather similar to SCS-MP2.

2.1.4 Basis set superposition error and counterpoise correction

The use of very high-level of theory does not automatically guarantee that a quantitative description of weak interactions is obtained.[27] Significant error can be introduced to the results if the employed basis set is insufficient. Most notably, the employed basis set must be at least valence triple-ζ in quality and augmented with both polarization and diffuse functions. Diffuse functions are particularly important since they allow better description of electron correlation effects at the far edges of the electron density distribution. Even if sufficiently large basis set are employed, significant error in the results can arise from basis set superposition error (BSSE).[53] BSSE stems from the fact that the orbital basis sets of individual molecules A and B (monomers) are simultaneously used to describe the orbital basis set of the intermolecular assembly (dimer) at finite separation (Figure 1).[29] As a consequence, the interaction energy of the intermolecular assembly is estimated too small and the interaction distance is described overly short.

The simplest way to treat BSSE is to use an extended basis set that is close to the complete basis set (CBS) limit.[54] A common *a posteriori* way to treat BSSE is the counterpoise correction (CP) that requires two additional energy calculations $E_A(X_{AB})$ and $E_B(X_{AB})$ in the dimer basis for monomers A and B, respectively.[29,30] In these calculations, the atoms of the other monomers are treated as ghost atoms, that is, only their basis functions, but not their nuclei or electrons, are present (see Figure 1). By subtracting the energies $E_A(X_{AB})$ and $E_B(X_{AB})$ from the standard energies $E_A(X_A)$ and $E_B(X_B)$ of the individual monomers, the counterpoise correction is obtained

$$\delta^{CP} = [E_A(X_A) + E_B(X_B)] - [E_A(X_{AB}) + E_B(X_{AB})]. \quad (2.2)$$

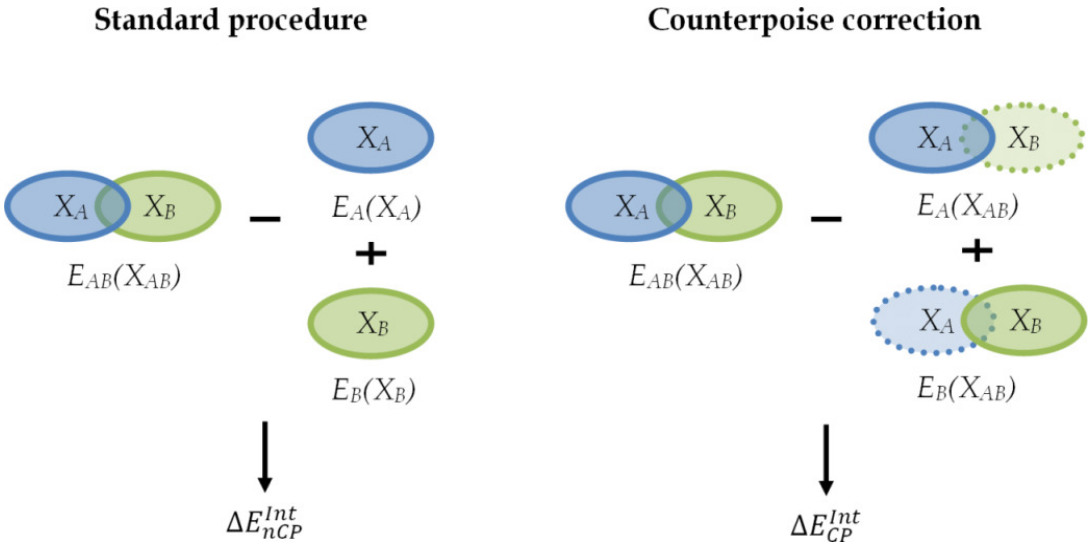

Figure 1. The standard (left) and counterpoise corrected (right) method for calculating the interaction energy of two weakly interacting molecules A and B. The standard method leads to interaction energy (ΔE_{nCP}^{Int}) that is too small and, consequently, to an intermolecular distance that is too short. This arises because the dimer AB has twice the amount of primitives to describe the interaction as compared to the basis sets of the individual monomers. The counterpoise correction procedure yields better interaction energies (ΔE_{CP}^{Int}) as the energies of the individual monomers A and B are calculated in the orbital basis of the dimer. The monomers A (blue) and B (green) and their orbital basis sets X_A and X_B are illustrated by ellipsoids. The ghost monomers A and B are marked with a dotted line and background.

In addition, if the standard interaction energy is defined as

$$E_{nCP}^{Int} = E_{AB}(X_{AB}) - [E_A(X_A) + E_B(X_B)], \tag{2.3}$$

then the counterpoise corrected interaction energy is given by Equations 2.4 and 2.5

$$E_{CP}^{Int} = E_{nCP}^{Int} + \delta^{CP} \tag{2.4}$$

$$E_{CP}^{Int} = E_{AB}(X_{AB}) - [E_A(X_{AB}) + E_B(X_{AB})]. \tag{2.5}$$

Even though the CP correction requires additional energy calculations, it is a practical and simple approach for correcting the interaction energies of molecular assemblies. However, the CP correction cannot be used to correct BSSE from systems with weak intramolecular interactions. These interactions are especially important in large biological systems and there has been a growing interest in the development of methods which can treat not only intermolecular but also intramolecular BSSE.[55] An example of such methods is the semi-empirical CP correction a.k.a. geometrical counterpoise (gCP)[55a] that considers the contributions of the individual atoms to BSSE. An alternative is the atomic

CP method whose fundamental idea is rather similar to gCP.[55b] Alternatively, DFT methods with augmented dispersion correction can also be used to eliminate both intra- and intermolecular BSSE as the density functional formalism is by itself characterized by negligible BSSE.[55c]

CP correction has also received some criticism because it violates the Pauli exclusion principle.[29] This can be easily explained with the following example. When the energy of the monomer A is calculated in the dimer basis and the atoms of the monomer B are treated as ghost atoms, the monomer A has more basis functions available than in the conventional calculation. In particular, certain basis functions which would have been occupied by the electrons of the monomer B now become available for the electrons of the monomer A. Thus, the Pauli exclusion principle is violated, which can in some cases lead to overcorrection of BSSE. Such overcorrection is a particular problem in hydrogen-bonded systems,[56] whereas for dispersion dominated systems the CP procedure typically yields superior results.[57]

In addition to BSSE, all quantum chemical calculations suffer from the basis set incompleteness error (BSIE).[29] BSIE arises from the fact that most of the currently used basis sets are too small to describe the systems of interest and therefore yield results which deviate significantly from the CBS limit. Because BSSE and BSIE have different signs, some error cancellation takes place and artificially good results can be obtained from calculations employing small basis sets and no CP correction.

2.1.5 Local correlation methods

Local correlation methods (LCMs) were originally developed to reduce the steep dependence of the computational cost on the size of the chemical system, but they also introduce another approach to obtain BSSE free energies and geometries as they avoid the pitfalls of their canonical equivalents by employing local orbital spaces to restrict the number of excited determinants in the wave function.[31] The restriction allows linear scaling of the methods and calculations can be accelerated by applying density fitting.[vii] Thus, even the highest level methods such as LCCSD(T) can be used to describe molecules with 50 to 100 atoms.[31,58]

The standard procedure of local correlation methods includes a number of key steps. First, the occupied molecular orbitals (MOs) are localized by using the standard localization procedures such as Boys,[59] Pipek-Mezey[60] or natural orbitals[61] to obtain localized molecular orbitals (LMOs).[31,61b] On the other hand, the virtual space is spanned by nonorthogonal atomic orbitals (AOs) which are projected against the occupied orbitals to ensure orthogonality between occupied and virtual spaces.[31] Overall, this procedure gives fully localized projected atomic orbitals (PAOs). Second, for each correlated LMO the specific orbital domain is generated by employing a Bought and Pulay procedure.[62] The orbital

[vii] In the density fitting approximation, the 4-index two-electron integrals are approximated by products of 2-index and 3-index integrals.

domain includes every single PAO that is generated from all AOs of those atoms that significantly contribute to the LMO.[31] Once the LMOs and their corresponding domains are formed, excitations are allowed only between LMOs and their corresponding domains. This approach significantly decreases the amount of excited configurations in the wave function and thereby lowers the computational cost. Furthermore, if the domains of monomers are determined at large intermolecular distance and kept fixed throughout geometry optimization, virtually BSSE free energies and geometries are obtained for the dimer because each monomer only contains PAOs from its own basis. Naturally, somewhat less correlation energy is recovered due to restrictions in the allowed excitations, but the accuracy of the LMOs can be affected by either extending the domains or introducing unions of domains for including double and triple excitations. In the former method, the standard domains are extended by adding PAOs centered at neighboring atoms, whereas in latter method the domains are formed as a union of either two or three domains for double and triple excitations, respectively.

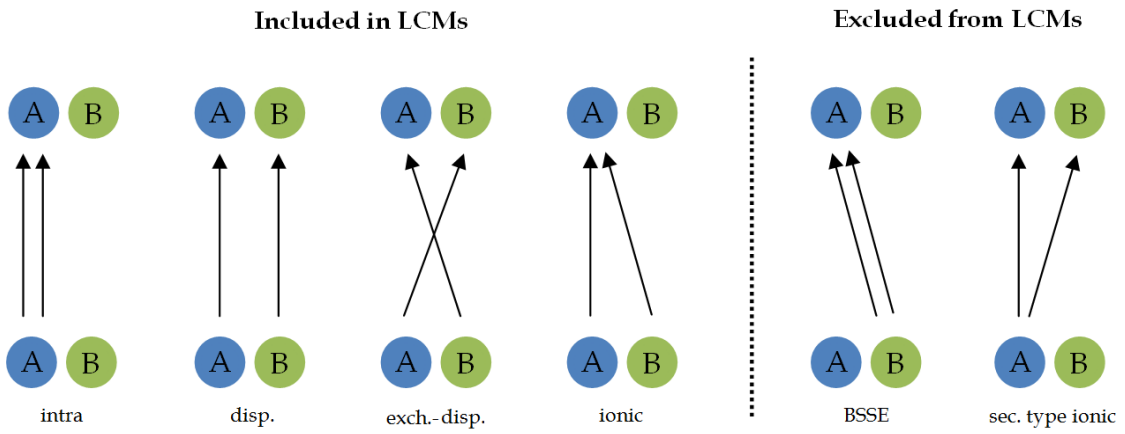

Figure 2. An illustrative example of how the intermolecular interaction energy of a dimer can be partitioned to different double excitation classes in local correlation methods (LCMs).[63] The blue and green circles represent the monomers A and B, respectively, in their ground (lower) and excited (upper) state. The vertical arrows correspond to excitations.

In addition to BSSE free energies, the local correlation methods also allow partitioning the intermolecular interaction energy of the dimer to different excitation classes (intramolecular correlation, dispersion, exchange dispersion and ionic contribution) which can reveal important information about its physical origin.[31,viii] This is illustrated pictorially in Figure 2 with the help of double excitations.[31,63] Intramolecular correlation is the only class which describes simultaneous excitations within one monomer. That is, the electrons are excited from the LMOs of the monomer to the virtual space of the same monomer. All other excitation classes include simultaneous excitations either from both monomers

[viii] It should be noted that the partitioning scheme in local correlation methods is only valid as long as the orbital domains of the two monomers do not overlap.

to their own virtual space (dispersion) or cross-excitations from one monomer to the virtual space of the other monomer (ionic and exchange-dispersion). In addition to the allowed excitations, two types of excitations are excluded from the local correlation methods. These are the double cross-excitations from one monomer to the virtual space of the other monomer and the second of ionic excitations. The former are basically responsible for BSSE and should be omitted, whereas the latter produce only a small contribution to the interaction energy.

Local correlation methods are not the only available methods that allow decomposition of the interaction energy according to different excitation classes. A rather similar analysis can be done by using the supermolecular approach within the symmetry-adapted perturbation theory (SAPT).[64,65] The fundamental idea of SAPT is that the interaction energy of two isolated monomers is treated as quantities originating from the mutual perturbation of the two monomers. Since the interaction energy can be written as a sum of different terms (the electrostatic, inductive, exchange and dispersive components), SAPT provides physical insight to the interaction between two monomers. The differences and similarities between SAPT and local correlation methods are discussed in more detail in the literature,[66] but, in general, SAPT is computationally more demanding than local correlation methods when post-HF wave functions are employed.[66] However, SAPT can also be combined with the DFT formalism of electron structure theory, which has made it a rather popular method for the study of different intermolecular interactions.[38]

2.2 Results and discussion

2.2.1 $X_3Pn\cdots PnX_3$ dimers (Pn = N-Bi; X = F-I)

Lately, Ganesamoorthy *et al*. reported the crystal structure of the aminotetra(phosphine) ligand p-$C_6H_4[N(PCl_2)_2]_2$ (**1**) in which short intermolecular contacts exist only between tri-coordinated phosphorus atoms (-$NCl_2P\cdots PCl_2N$- = 3.54 Å), indicating that the attractive dispersion force has a strong influence on the solid state packing of this compound (Figure 3).[67] The attractive nature of the P···P interaction was supported by preliminary theoretical calculations for a model system $Cl_3P\cdots PCl_3$, which pointed out that the interaction is weak but binding. Interestingly, the solid state packing of the fluorine analogue of **1** was found to be different and, instead of P···P interactions, dominated by electrostatic intermolecular F···H, F···P and F···C contacts. The absence of P···P interactions in the fluorine analogue of **1** was also confirmed by computational analysis.

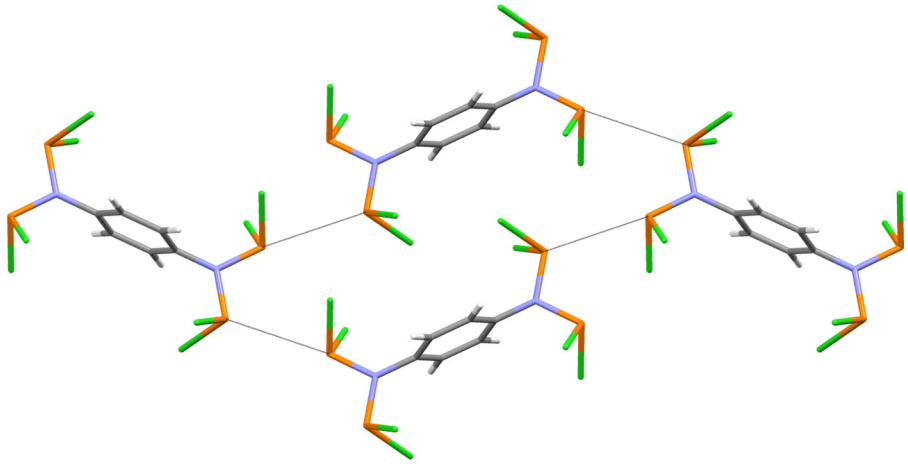

Figure 3. Intermolecular P···P interactions in compound **1.**

Compound **1** is not the only example in which intermolecular interactions are observed between halogenated tri-coordinated pnictogen moieties of the type -PnX_2 (Pn = pnictogen; X = F, Cl, Br and I). An exhaustive search for different close Pn···Pn contacts (smaller than the sum of van der Waals radii) from the literature revealed that such interactions exist between all pnictogen atoms: -NF_2 (3.07 Å),[68] -PCl_2 (3.37 Å),[69] -AsI_2 (3.37 Å),[70] -$SbCl_2$ (3.67-3.83 Å)[71] and -$BiCl_2$ (3.89-3.98 Å).[71a] Analogous intermolecular interactions have also been observed for the fully halogenated pnictogen centers in SbF_3 (3.92 Å)[72] and $SbCl_3$ (3.78 Å).[73] Even though the presence of close Pn···Pn contacts in these structures has been noted in the literature, no speculation of their origin has been presented in any of the published results. In addition to the crystallographic data, spectroscopic measurements have shown that pnictogen trihalides PnX_3 (Pn = P, As, Bi; X = Cl, Br) can form ethane-like dimers in the liquid state.[74] Hence, taken as a whole, the tri-coordinated pnictogen moieties -PnX_2 and PnX_3 seem to have an intrinsic ability to form intermolecular interactions, but whether these interactions are strong enough to be used in crystal engineering was unknown. In the current work, an extensive computational analysis was carried out for the bifurcated C_{2h} symmetric model systems $X_3Pn\cdots PnX_3$ (**2-6**) to find an unambiguous answer to the question. The results of this study are presented in full in research Paper **I**.

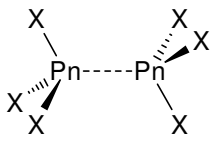

2 Pn = N **a X = F**
3 Pn = P **b X = Cl**
4 Pn = As **c X = Br**
5 Pn = Sb **d X = I**
6 Pn = Bi

The relatively weak nature of the Pn···Pn interaction in **2-6** is revealed at the CP corrected HF level of theory which predicted all of the studied dimers to be unbound (Table 1). The inclusion of dynamic electron correlation via perturbation theory changed the picture dramatically and CP corrected MP2 and LMP2 yielded very similar results, predicting 10 of the studied dimers to be

true minima on the potential energy hypersurface. It needs to be noted here that the results at the conventional MP2 level differed considerably from CP-MP2 and LMP2 data, mainly due to the tendency of MP2 to overestimate the strength of the Pn···Pn interaction.[27] This led to abnormally short Pn···Pn distances in all studied systems as well as to location of some unphysical transition states (**2c** and **2d**). The fact that the Pn···Pn distances were calculated to be around 0.05 Å longer at the LMP2 level of theory than using CP-MP2 can be attributed to the formalism employed in the local correlation method which limits the number of excitations.[31] Furthermore, one of the ionic components is totally excluded from the LMP2 approach, which decreases the amount of recovered electron correlation even more.

Table 1. Calculated E···E distances [Å] in $X_3Pn\cdots PnX_3$ dimers (**2**-**6**) and the electronegativity difference of atoms Pn and X (X_{Pn}-X_X) in the Pauling scale.

	r(E···E)				
	PBE-D	MP2	CP-MP2	LMP2	X_{Pn}-X_X
2a	3.13	3.00	3.14	3.14	-0.94
2b	3.02	2.80	2.90	2.92	-0.12
2c	2.92	2.64[a]	2.81	2.84	0.08
2d	2.84[a]	2.48[a]	2.67	2.69	0.38
3b	3.35	3.17	3.27	3.36	-0.97
3c	3.01	2.90	3.09	3.18	-0.77
3d	2.81	2.57	2.80	2.91	-0.47
4b	-	3.27	-	-	-0.98
4c	3.73[a]	3.07	3.34	3.42	-0.78
4d	3.07[a]	2.85	3.10	3.16	-0.47
5c	-	3.81	-	-	-0.91
5d	3.88	3.30	3.79	3.84	-0.61
6d	-	3.58	-	-	-0.64

[a] Transition state on the potential energy hypersurface.

The standard exchange-correlation functionals cannot describe the non-local dispersion force due to their local nature.[34] Therefore, it was expected that neither PBE0 nor TPSSTPSS replicates the results obtained at the CP-MP2 and LMP2 levels of theory. The hybrid PBE0 method predicted only three of the dimers (**3c**, **3d** and **5d**) to be minima on the potential energy hypersurface, whereas only two minima (**2c** and **3c**) were located with the TPSSTPSS functional. These findings reflect the fact that standard density functionals are not designed to take into account the dispersion force. The performance of the PBE0 and TPSSTPSS functionals could have been improved by introducing the DFT-D3 correction, but unfortunately this was not available at the time of the original investigations. Consequently, the older and more empirical version, namely DFT-D2, was used to correct the PBE functional for dispersion (PBE-D). This

approach yielded much better results than either of the two standard functionals and gave similar Pn···Pn bond lengths for nitrogen and phosphorus dimers as LMP2 (Table 1). However, the PBE-D results for the heavier analogues deviated significantly from the LMP2 and CP-MP2 data, and the used functional predicted all of these dimers to be transition states, indicating possible inefficiencies in the atomic parameterization within the DFT-D2 method.

To summarize, geometry optimizations at the CP-MP2 and LMP2 levels of theory indicated clearly that weak Pn···Pn interactions exist within the studied dimers **2-5**. Furthermore, the acquired data revealed another interesting phenomenon: the number of stable minima found decreases by one at each consecutive step when going down the pnictogen group (Table 1). This could be explained with the electronegativity difference between the halogen (X) and pnictogen (Pn) atoms. As the electronegativity difference increases, so does the polarization of the Pn-X bond and once sufficiently strong, it will lead to a repulsive $Pn^{+\delta}\cdots{}^{+\delta}Pn$ interaction between the monomers. As Table 1 shows, if the electronegativity difference stays roughly within ±1 at the Pauling scale, the Pn···Pn interaction remains attractive in most of the systems studied.[ix] Consequently, nitrogen was the only one of group 15 elements that was found to form stable dimers in combination with all halogens.

Table 2. Interaction energies [kJ mol^{-1}] of dimers **2-5**.

	CP-MP2	LMP2	PBE-D	SCS-LMP2	LCCSD(T)
2a	-3	-3	-4	-2	-3
2b	-16	-15	-9	-9	-11
2c	-22	-21	-15	-12	-13
2d	-33	-31	-24[a]	-17	-13
3b	-15	-13	-11	-8	-9
3c	-24	-21	-18	-11	-12
3d	-42	-36	-31	-19	-15
4c	-20	-16	-18[a]	-8	-9
4d	-36	-31	-29[a]	-17	-15
5d	-26	-24	-35[a]	-13	-14

[a] Transition state on the potential energy hypersurface.

To gain more insight into the Pn···Pn interaction, the interaction energies of dimers were calculated at the SCS-LMP2 and LCCSD(T) levels of theory employing geometries optimized at the LMP2 level. As seen from Table 2, the different methods yield a qualitatively similar picture of the interaction. That is, the calculated interaction energies of dimers decrease as the softness of the halide X increases. Thus, the most strongly bound systems are the iodine species

[ix] The only exceptions are **4b** (X_{As}-X_{Cl} = -0.98), **5c** (X_{Sb}-X_{Br} = -0.91), **6c** (X_{Bi}-X_{Br} = -0.94) and **6d** (X_{Bi}-X_{I} = -0.64). These can be partly explained by the fact that the valence shell electrons of heavy nuclei are more diffuse and the corresponding Pn-X bonds are therefore more easily polarized despite smaller difference in electronegativity.

2d, **3d** and **4d**. This result is fully on par with earlier computational works in which the interaction energy of a metallophilic attraction in perpendicular $[XAuPR_3]_2$ dimers was observed to increase in a similar fashion.[63] Even though CP-MP2 and LMP2 give qualitatively similar results to LCCSD(T), their tendency to overestimate the strength of the dispersion force led to large quantitative differences (Table 2).[27a] This was, however, corrected by spin component scaling, and as seen in Table 2, the SCS-LMP2 method gives interaction energies which are very close to the LCCSD(T) values. Based on these data, it can be concluded that the interaction energy in dimers **2**-**5** varies between -15 and -10 kJ mol^{-1}, which makes the investigated Pn···Pn interaction comparable in strength to that in $(H_2Pn\text{-}PnH_2)_2$[17d] as well as to the π···π and CH···π interactions between two benzene molecules.[27a]

The PBE-D functional predicted Pn···Pn interaction energies between LMP2 and LCCSD(T) data for **2** and **3**, whereas the energies for the heavier dimers **4** and **5** were closer to the CP-MP2 and LMP2 results. The apparent overestimation of the strength of the interaction between the heavier group 15 elements was a rather interesting result since the PBE-D functional described these dimers to be transition states on the potential energy surface.

The local correlation formalism allows the decomposition of the interaction energy into physically meaningful classes. This kind of energy partitioning for dimers **2**-**5** unambiguously confirmed that the Pn···Pn interaction originates from the dispersion force. The analysis also showed that the interaction contains an important ionic component whose importance increases with increasing atomic size. As a matter of fact, the magnitudes of the ionic (35.8 kJ mol^{-1}) and dispersion (45.1 kJ mol^{-1}) contributions in the most strongly bound dimer **3d** were close to the values typically observed in aurophilic interactions, even though the calculated total interaction energy is much smaller in **3d**.[63] However, the aurophilic interaction is strengthened by relativistic effects,[18] which readily explains the difference from the investigated Pn···Pn interactions.

2.2.2 Homopolyatomic chalcogen dications Ch_8^{2+} (Ch = S or Se)

The physical origin of weak transannular chalcogen···chalcogen (Ch···Ch) interactions in inorganic ring systems has puzzled both computational and experimental chemists for a long time.[75,76,77,78] These interactions exist both in heterocyclic rings (see Section 3.3.1)[78,79,80] as well as in homopolyatomic cations.[75a,81] An archetypical example of the latter species is the octasulfur dication S_8^{2+} (**7a**) that has an overall chair-like molecular shape with one weak transannular Ch···Ch interaction (Figure 4).[75a] The heavier chalcogen analogues of **7a** are also known and they have similar molecular structures with one weak transannular Se···Se or Te···Te interaction.[81]

The length of the Ch3···Ch7 interaction in chalcogen dications **7** is clearly elongated if compared to typical S-S (2.06 Å) and Se-Se (2.32 Å) single bond lengths, which indicates that a closed shell attraction (dispersion) might exist between atoms Ch3 and Ch7. On the other hand, a qualitative picture of bonding interactions in **7** can be obtained using Gillespie's rules, developed for main

group cage and cluster systems, which signify that the Ch3···Ch7 interaction should be covalent in its origin.[76b] Moreover, the atoms in molecules (AIM) analysis revealed a bond critical point within the Ch3···Ch7 bond path in all Ch_8^{2+} dications, which further underlines the covalent character of this interaction.[75a] The results from AIM analyses were supported by detailed spectroscopic studies of **7a** which revealed a Raman stretch associated with the transannular S3···S7 bond.

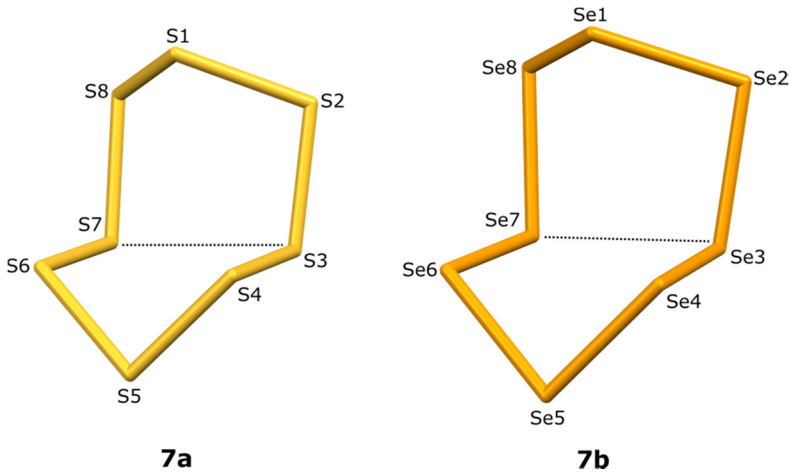

Figure 4. The chair-like molecular structures of S_8^{2+} (**7a**) and Se_8^{2+} (**7b**) with one weak Ch3···Ch7 cross-ring interaction. Average experimental bond lengths: r[S3···S7] = 2.859(3) Å and r[Se3···Se7] = 2.950(4) Å.[75a,81b]

If the Ch3···Ch7 interaction in **7** is primarily covalent in nature, HF should be able to describe it with sufficient accuracy. Nevertheless, the HF method was shown to give an overly short Ch3···Ch7 distance for both S_8^{2+} and Se_8^{2+}, indicating that they should possess a classically σ-bonded bicyclic structure.[75b] Any attempt to improve the HF results by treating dynamic electron correlation with MPPT led to a significant (up to 1 Å) overestimation of the Ch3···Ch7 interaction in both dications,[75b] which suggests that the transannular interaction in these systems cannot originate solely from closed shell interactions.[27,82]

Ciolowski and Gao were the first to conduct a more detailed theoretical analysis of **7a** and **7b** using localized natural orbitals (NOs) at the MP2 level.[75b] This revealed that a significant amount of electrons in the wave functions of **7** are transferred from the formally occupied orbitals to the virtual space. Thus, it was concluded that the wave functions of octachalcogen dications most likely contain multiconfigurational character. Unfortunately, no higher-level calculations could be performed due to the computer hardware limitations at the time.

If the electronic wave functions of Ch_8^{2+} dications truly contain some amount of multiconfigurational character, DFT methods would be expected to be able to describe their geometries in a reasonable fashion.[x] Nevertheless, the performance of different density functionals has been highly varied.[75] For ex-

[x] For a more detailed discussion about the performance of DFT in describing multiconfigurational character, see Section 3.2.1.

ample, the MPW91MPW91 functional provided exceptionally accurate geometries for both dications,[75a] whereas the BLYP exchange-correlation functional performed very poorly and predicted significantly elongated cross-ring interaction in S_8^{2+}.[75b]

Owing to the inconsistencies in the theoretical results and the lack of high-level calculations for any Ch_8^{2+}, it can be concluded that a solid physical explanation of their weak Ch3···Ch7 interaction had not yet been presented. Thus, an extensive quantum chemical study of the dications was conducted which confirmed the complexity in their electronic structures. The results from these investigations were reported in full in the original research Paper **II**.

The structures of S_8^{2+} and Se_8^{2+} were first optimized in the gas phase with different single determinant methods (HF, MPPT, QCISD(T), CCSD(T) and DFT). All of the employed methods predicted Ch-Ch bond lengths in good agreement with the experimental data but they gave highly varying results for the Ch3···Ch7 contact (Figure 5). The HF and MP2 methods performed similarly to what has been described before and predicted the Ch3···Ch7 interaction either too short or too long, respectively.[75b] Interestingly, HF level calculations for the triplet state gave lower energy solutions for both dications. The performance of MPPT could be improved by considering correlation effects to the third order (MP3), but the addition of fourth order terms (MP4) led again to a substantial elongation of the Ch3···Ch7 contact in both systems studied. The QCISD(T) and CCSD(T) methods were the only single determinant *ab initio* approaches which were able to predict the Ch3···Ch7 distances in S_8^{2+} and Se_8^{2+} in good agreement with the experimental data.

DFT-based methods showed varying performance with one clear trend: the Ch3···Ch7 contact became shorter whenever the amount of exact exchange used in the functional increased. From all of the density functionals employed, PBE0 performed the best and gave geometrical parameters that outperformed even QCISD(T) and CCSD(T). It was also noted that the inclusion of empirical dispersion correction (DFT-D3) improved the description of the Ch3···Ch7 contact only slightly. This finding was consistent with the earlier notion that the dispersion force does not determine the observed transannular interaction.

The crystal structures of both S_8^{2+} and Se_8^{2+} contain several short cation-anion contacts that could potentially have a strong influence on the geometries of the cations.[75a,81b,c] If the observed Ch3···Ch7 distances are long simply due to secondary bonding interactions, the comparison of calculated gas phase geometries to the X-ray data is not justified. Thus, it was important to ensure that the theoretical methods predicted comparable structures for octachalcogen dications both in the gas phase and in the solid state. This was confirmed by running solid state calculations at the HF, B3LYP, PBE and PBE0 levels of theory for S_8^{2+}. The results showed that all of the employed methods performed similarly as in the gas phase, which supports the view that secondary bonding interactions do not play a significant role in determining the transannular distances, thereby validating comparisons between gas phase and X-ray data.

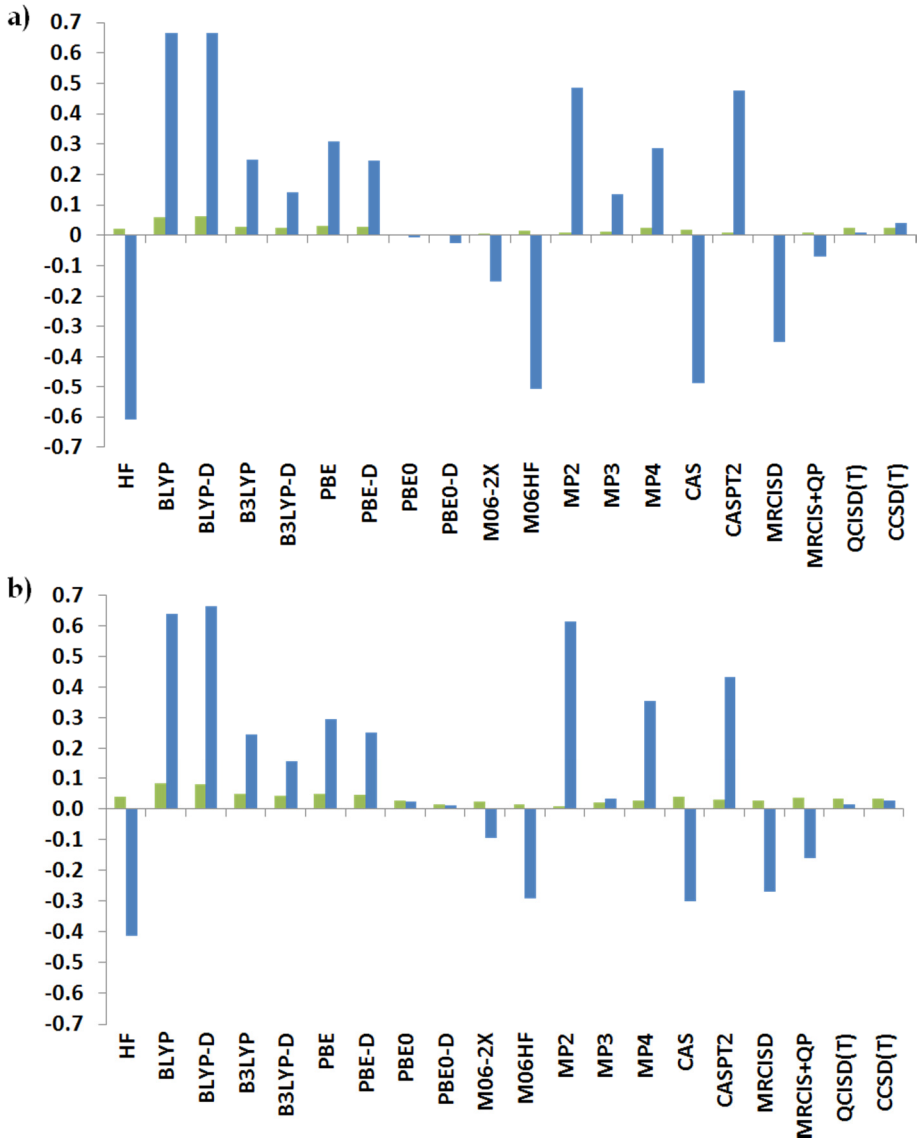

Figure 5. Deviations between the calculated and experimental bond lengths [Å] for (a) S_8^{2+} and (b) Se_8^{2+}.[75a,81b] All data calculated in the gas phase. Color code: Ch-Ch bond lengths (green), Ch···Ch (blue).

Before the wave functions of octachalcogen dications were modeled using multiconfigurational methods, NO analyses were performed for the optimized geometries at the QCISD(T) level of theory.[xi] The analyses showed that both dications have several NOs whose occupation is either notably lower than 2 or higher than 0, supporting the existence of strong electron correlation effects.[75b] Most importantly, the NOs of S_8^{2+} (Se_8^{2+}) that are bonding and antibonding with respect to the Ch3···Ch7 interaction were found to have fractional occupations of 1.86 e^- (1.87 e^-) and 0.20 e^- (0.19 e^-), respectively (Figure 6). This not only offered an explanation for the elongation of the Ch3···Ch7 bonds but it also indicated that the HOMO-1 to LUMO excited determinant could be important in

[xi] For a more detailed discussion about NO analysis, multiconfigurational methods and static electron correlation, see Chapter 3.

recovering the correlation effects. However, even though this determinant was specifically included in the complete active space (CAS) wave function, the calculations did not lead to any significant improvement of the results (Figure 5). Furthermore, the inclusion of dynamic electron correlation via second order perturbation theory (CASPT2) or by multireference configuration interaction (MRCI) yielded varying results. These data clearly showed that static electron correlation effects do not play a key role in the electronic structures of Ch_8^{2+}.

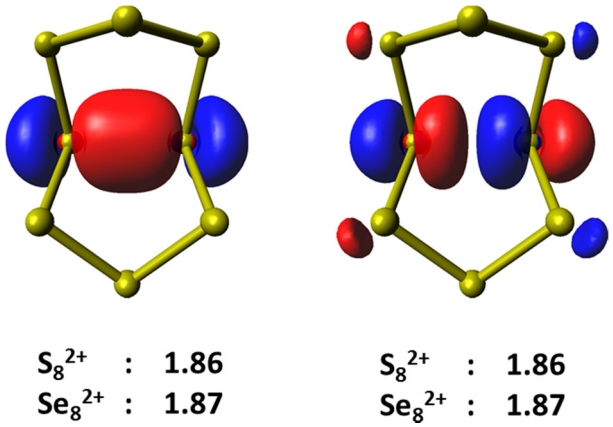

Figure 6.The most important fractionally occupied QCISD(T) natural orbitals of E_8^{2+} along with their occupancies.

Having established that the transannular interactions in Ch_8^{2+} originate from dynamic correlation other than dispersion, the role of different excited determinants in the overall picture was investigated by optimizing the geometry of S_8^{2+} at the CISD, QCISD and CCSD levels of theory. The CISD approach does not take into account the disconnected double excitations and it gave a very short S3···S7 distance of 2.362 Å.[25] The addition of four-electron correlation effects via QCISD and CCSD lengthened the S3···S7 distance to 2.572 Å and 2.627 Å, respectively, indicating that the effect of disconnected terms is significant. A comparison of these data to the most accurate CCSD(T) level calculations further showed that the triple excitations contribute approximately the same amount to the S3···S7 interaction as the disconnected double terms.

In light of all of the above data, it could be concluded that the transannular interactions in Ch_8^{2+} originate from covalent bonding which becomes significantly elongated and weakened due to strong and complex dynamic electron correlation effects arising from disconnected double and higher excitations. Thus, a large and balanced set of determinants is needed to obtain an accurate description of the electronic structures of octachalcogen dications. Consequently, when all of the essential electron correlation effects are taken into account either using QCISD(T) or CCSD(T), the transannular interactions are predicted in good agreement with the X-ray data.

2.2.3 RTlTlR dithallenes (R = alkyl, aryl)

In the 1970s, Lappert *et al.* synthesized the novel tin(II) alkyl dimer $\{Sn[CH(SiMe_3)_2]_2\}_2$ that was found to have a weak Sn=Sn double bond in the solid state.[83] The compound was kinetically stabilized using sterically encumbered ligands and was considered to be the first one to have a formal multiple bond between two heavy main group elements under ambient conditions. Since the discovery of this compound, sterically encumbered ligands have been used to stabilize a plethora of other compounds that contain homonuclear multiple bonds between heavier group 14 and 15 elements.[84]

It was long thought that group 13 elements cannot form homonuclear multiple bonds due to their electron-deficient nature. It has, however, later been observed that even the heaviest group 13 element thallium can form a homonuclear "double" bond in RTlTlR, provided that large enough substituents are used (R = C_6H_3-2,6-(C_6H_3-2,6-Pr^i_2)$_2$).[85] However, in this compound, the metal-metal bond is actually slightly elongated (3.09 Å) compared to a typical Tl-Tl single bond (2.88 Å) and the -CTlTlC- core adopts a planar trans-bent (not linear) structure. It was also found that the dimer readily dissociates into monomers in solution, which underlines the weak nature of its Tl-Tl bond.

From a theoretical point of view, the nature of multiple bonding in all group 13 dimetallenes and their dianions has often been explained with the contribution from the "slipped" π-type orbital which is the highest occupied molecular orbital (HOMO) in dimetallenes.[5] If this orbital truly has metal-metal bonding character, its effects should be visible already at the HF level of theory. However, in case of dithallenes, the above explanation can be immediately excluded since HF predicts the parent species HTlTlH to be unbound.[6] This strongly suggests that the bonding interactions in dithallenes are not covalent, but resemble more closed shell interactions between Tl(I) monomers.[86] Clearly, the existing theoretical evidence offers no support for a double bond in the parent dithallene. It was therefore of interest to have a closer look at the electronic structures of the model systems **8** with more realistic substituents. The results of this study are presented in full in research Paper **III**.

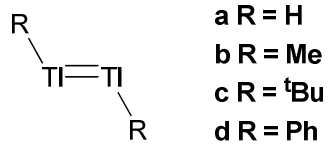

8

a R = H
b R = Me
c R = ^{t}Bu
d R = Ph

As expected based on earlier theoretical results, all studied dithallenes were found to be unbound at the HF level of theory.[6] A dramatic change to this picture was observed when dynamic electron correlation effects were treated either with MP2 or CCSD(T). Both of these correlated methods predicted Tl-Tl distances which were in reasonable agreement with the experimental data, indicating that a closed shell metal-metal attraction plays an important role in the

electronic structures of all dithallenes. Even though a detailed analysis of the results did not give any indication of static electron correlation in these systems, CAS and CASPT2 calculations were nevertheless performed as the wave functions of their lighter aluminum and gallium analogues were shown to possess some diradical character (see Section 3.3.2). Geometry optimizations at the CAS level gave structures in which the Tl-Tl distance was strongly elongated and, in fact, **8d** was not even bound at this level. These results were significantly improved by inclusion of dynamic electron correlation via perturbation theory (CASPT2), which yielded similar geometries to MP2 and CCSD(T) for **8**.

The consistency of the results at the MP2, CCSD(T) and CASPT2 levels confirmed that the thallium-thallium bond in dithallenes originates solely from dynamic electron correlation effects and dispersion in particular. An energy analysis at the CCSD(T) level further augmented this view and showed that the interaction energies of **8a** and **8b** are around -10 kJ mol^{-1}, which is considerably less than the typical energy of a Tl-Tl single bond (≈164 kJ mol^{-1}).[xii]

[xii] The single bond energy was evaluated by calculating the dissociation energy of Tl-Tl bond in H_2Tl-TlH_2.

3 MULTICONFIGURATIONAL CHARACTER IN MAIN GROUP SYSTEMS

Electron correlation effects are generally divided into two categories, dynamic and static, of which the latter can also be called non-dynamic electron correlation.[23] Dynamic electron correlation refers to the correlated motion of electrons which arises from their instantaneous mutual repulsion. This kind of electron correlation is particularly important for molecular assemblies interacting via non-covalent interactions.[xiii] In contrast to dynamic electron correlation, static electron correlation stems from the degeneracy or near degeneracy of different electronic configurations. In other words, a molecule or atom has multiconfigurational character in its wave function. A representative and common chemical phenomenon that involves static electron correlation is the homolytic dissociation of covalent bonds. Multiconfigurational character is also present at the wave functions of main group singlet diradicals.[87]

Diradicals have two unpaired electrons that occupy two degenerate or nearly degenerate molecular orbitals (MOs), and depending on the interaction of these electrons, they can form either a singlet or a triplet state via antiferromagnetic or ferromagnetic coupling, respectively.[88] Owing to this, they are a class of compounds that has gained considerable amount of visibility since the understanding of their spin interactions can lead to creation of novel materials that could be used as suitable building blocks for spintronics (spin-based electronics) which utilizes electron spin for encoding and transmitting information.[89]

For a long time, triplet state diradicals were more extensively studied than singlet diradicals because they have longer lifetimes. It was also thought that singlet diradicals exist only as transition states and short-lived intermediates in chemical reactions.[88] However, the synthesis of 2,4-diphosphacyclobutane-1,3-diyl by Bertrand *et al.* in 1995 was a major breakthrough in the field of stable singlet diradicals and it initiated a new strategy to stabilize main group singlet diradicals.[90] Currently, a plethora of different main group singlet diradicals are

[xiii] For a more detailed discussion about dynamic electron correlation, see Chapter 2.

known of which many are based on the same structural motif as 2,4-diphosphacyclobutane-1,3-diyl.[87] Although their increased stability decreases diradical character, they are potentially applicable as initiators for radical reactions, as radical scavengers[91] and as starting materials for antiferromagnetic low-spin polymers exhibiting metallic conductivity.[92]

Since the wave functions of singlet diradicals contain (near) degeneracy effects, they must be described using high-level multiconfigurational methods if quantitative accuracy is sought.[23,93] The use of sophisticated computational approaches has not only given insight into their complex electronic structures but it has also increased our understanding of the nature of chemical bonding in general.[87] For example, together with experimental results, quantum chemical calculations have proven that a short interatomic distance is not necessarily a sign of covalent bonding or strong interaction between two radical sites.

In the following two subchapters, the theory behind multiconfigurational character and singlet diradicals is first introduced. Then the qualitative and quantitative performance of different quantum chemical methods in describing static electron correlation effects is briefly reviewed. The results and discussion part reports two specific case studies which are discussed in full in research Papers **II** and **III**. The original research Paper **II** reports on the multiconfigurational character of tetrachalcogen tetranitirides, whereas in research Paper **III**, the electronic structures and singlet diradical character of group 13 dimetallenes are examined.

3.1 Multiconfigurational wave functions and diradicals

Multiconfigurational character of wave function is often connected with bond breaking and formation processes in which MOs dissociate or merge in order to form new MOs.[23,93] By no means is multiconfigurational character restricted to these processes as even the electronic ground states of many molecules or atoms include (near) degeneracy effects. Particularly, the wave functions of molecules containing transition metals are often dominated by static electron correlation effects as different electronic configurations have very similar energies.[93] The excited states of molecular systems also usually have strong configurational mixing, which leads to multiconfigurational wave functions. None of the aforementioned situations can be described by using the HF approach and a single Slater determinant, which makes the use of more sophisticated quantum chemical methods mandatory.[23,93] In this respect, it is illustrative to examine the dissociation of a hydrogen molecule, H_2, as an example of a system whose treatment requires the use a multiconfigurational wave function.

By using a minimal basis set and omitting the normalization constant and spin function, the restricted Hartee-Fock (RHF) wave function of H_2 can be written in terms of a single Slater determinant

$$\Psi_1 = \Psi_{RHF} = \psi_1(\boldsymbol{r}_1)\psi_1(\boldsymbol{r}_2), \tag{3.1}$$

where $\psi_1 = \chi_A + \chi_B$ is the bonding MO built from s-type AOs χ_A and χ_B located at the nucleus A and B, respectively, and $\mathbf{r}_1$ and $\mathbf{r}_2$ are the spatial coordinates of electrons 1 and 2, respectively.[93] By expanding the MOs in the above wave function as products of AOs, Equation 3.1 can be written in the following form

$$\begin{aligned}\Psi_{RHF} &= [\chi_A(\boldsymbol{r}_1) + \chi_B(\boldsymbol{r}_1)][\chi_A(\boldsymbol{r}_2) + \chi_B(\boldsymbol{r}_2)] \\ &= \chi_A(\boldsymbol{r}_1)\chi_A(\boldsymbol{r}_2) + \chi_A(\boldsymbol{r}_1)\chi_B(\boldsymbol{r}_2) + \chi_B(\boldsymbol{r}_1)\chi_A(\boldsymbol{r}_2) + \chi_B(\boldsymbol{r}_1)\chi_B(\boldsymbol{r}_2).\end{aligned} \tag{3.2}$$

The four terms can be rearranged

$$\Psi_{RHF} = [\chi_A(\boldsymbol{r}_1)\chi_B(\boldsymbol{r}_2) + \chi_B(\boldsymbol{r}_1)\chi_A(\boldsymbol{r}_2)] + [\chi_A(\boldsymbol{r}_1)\chi_A(\boldsymbol{r}_2) + \chi_B(\boldsymbol{r}_1)\chi_B(\boldsymbol{r}_2)] \tag{3.3}$$

to better illustrate that the RHF wave function of H_2 contains two terms in which electrons are located at separate nuclei as well as two terms in which both electrons are located at the same nucleus. These terms describe the covalent and ionic contributions to bonding, respectively, which means that the RHF wave function contains an equal amount of covalent and ionic character. At the equilibrium geometry, this is a reasonable approximation and the RHF approach gives a H-H bond distance which is close to the experimental value. However, upon dissociation, the ionic contribution gives an unphysical picture of bonding as it localizes both electrons to the same nucleus, giving one hydrogen atom with a positive charge (H^+) and one hydrogen atom with a negative charge (H^-). Since all covalent bonds dissociate homolytically, the unphysical ionic contribution must be removed from the wave function of H_2 when describing dissociation. This can be done by introducing a second Slater determinant (Ψ_2) into the total wave function of H_2 which takes into account the antibonding MO ($\psi_2 = \chi_A - \chi_B$).

The total multiconfigurational wave function (Ψ_{MC}) of H_2 can be constructed as a linear combination of two Slater determinants which have different coefficients C_1 and C_2 determining the weights of the determinants Ψ_1 and Ψ_2 in the total wave function,

$$\Psi_{MC} = C_1\Psi_1 + C_2\Psi_2.[93] \tag{3.4}$$

The multiconfigurational wave function Ψ_{MC} can be expanded in terms of AOs in a similar fashion to the RHF determinant

$$\begin{aligned}\Psi_{MC} &= C_1[\chi_A(\boldsymbol{r}_1) + \chi_B(\boldsymbol{r}_1)][\chi_A(\boldsymbol{r}_2) + \chi_B(\boldsymbol{r}_2)] \\ &\quad + C_2[\chi_A(\boldsymbol{r}_1) - \chi_B(\boldsymbol{r}_1)][\chi_A(\boldsymbol{r}_2) - \chi_B(\boldsymbol{r}_2)] \\ &= (C_1 - C_2)\,[\chi_B(\boldsymbol{r}_1)\chi_A(\boldsymbol{r}_2) + \chi_A(\boldsymbol{r}_1)\chi_B(\boldsymbol{r}_2)] \\ &\quad + (C_1 + C_2)[\chi_A(\boldsymbol{r}_1)\chi_A(\boldsymbol{r}_2) + \chi_B(\boldsymbol{r}_1)\chi_B(\boldsymbol{r}_2)].\end{aligned} \tag{3.5}$$

It can be clearly seen from Equation 3.5 that, by using the multideterminant wave function and varying the coefficients C_1 and C_2, not only the artificial ionic contribution can be removed during the dissociation process but also the whole potential energy curve of H_2 can be described correctly. Thus, at large separation, the coefficient C_2 will have roughly the same value but opposite sign than C_1 ($C_1 \approx -C_2$), whereas close to the equilibrium geometry $C_1 \approx 1$ and $C_2 \approx 0$ to remove the second Slater determinant from the wave function. During the bond breaking and formation process, the coefficients C_1 and C_2 adopt values in between these two extremes in order to give a good description of the potential energy curve.

3.1.1 Singlet and triplet diradicals

Diradicals are usually described by a two-electron two-orbital model.[87,88b,94] In a perfect diradical, the two MOs Φ_a and Φ_b are completely degenerate, orthogonal and they do not interact with each other. In such a case, two electrons can be placed in the two MOs Φ_a and Φ_b in six different electronic configurations of which three are singlet states and three are triplet states.[xiv] Because the three triplet states are equivalent in energy,[xv] a perfect diradical has four energy eigenstates: three singlets and one triplet. According to Hund's rule, the triplet state will be the most stable one, which is in agreement with the fact that pure diradicals often have a triplet ground state. However, there are some specific cases when a singlet state may fall below the triplet in energy. The relative ordering of the four possible states can be predicted by considering the overlap (S_{AB}), exchange (K) and Coulomb (J) integrals. The S_{AB} term describes the overlap between the MOs Φ_a and Φ_b, whereas J and K are two-electron operators describing the Coulomb electron-electron repulsion and the quantum mechanical exchange correction to the Coulomb repulsion energy, respectively.

In general, a strong overlap S_{AB} between two degenerate or nearly degenerate MOs Φ_a and Φ_b stabilizes one of the singlet states.[87,88b,94] If the overlap between these orbitals becomes large enough, the singlet state might fall below the triplet. However, the strong overlap of MOs will ultimately lead to bond formation and in such a case, MOs Φ_a and Φ_b form bonding and antibonding combinations. If the energy difference between these two orbitals is sufficiently large, the two electrons with opposite spins will occupy the lower energy orbital according to the Aufbau principle, which leads to a closed shell singlet state and to the total suppression of diradical character. Another case when the singlet state is favored over the triplet occurs when the two MOs Φ_a and Φ_b are not degenerate. In this case, the ground state multiplicity depends on the difference between the one-electron energies of the two MOs Φ_a and Φ_b. In order for

[xiv] Two of these configurations violate the indistinguishability of fermions. Therefore, the wave functions describing one of the singlet and triplet states must be formed as a linear combination of the two configurations.
[xv] This is true only in the absence of an external magnetic field and if the effect of the zero field splitting is neglected.

the singlet state to be favored, the difference must be greater than the exchange integral *K* between these MOs.

The last case when the energy of a singlet state might fall below the triplet is slightly different from two above examples.[87,88b,94] In case of triplet state diradicals, the spin parts of the two unpaired electrons are identical. Consequently, they cannot occupy the same MO as demanded by the Pauli exclusion principle. In singlet state diradicals, the two formally unpaired electrons have opposite spins and they can, therefore, be located in the same region of space without violating the Pauli exclusion principle. As a consequence, the electron-electron repulsion originating from the Coulomb integral is naturally weaker in a triplet state diradical than in a singlet state. However, when MOs Φ_a and Φ_b are disjoint, *i.e.*, they do not have atoms in common, the two electrons occupying these orbitals never appear in the same region of space, whether their spins are parallel or antiparallel. Due to this, the mutual electron-electron repulsion originating from the Coulomb integral is significantly lowered for a singlet state wave function. Furthermore, the exchange integral becomes virtually independent of the state multiplicity. As a result, the energy of the singlet state comes close to that of the triplet, in which case the multiplicity of the ground state is determined by the interactions of the two electrons occupying MOs Φ_a and Φ_b with the other electrons in the system. Hence, Hund's rule can be violated and the singlet state might become more stable than the triplet.

3.1.2 Quantification of singlet diradical character

Singlet diradical states play an important role in many chemical systems and phenomena: in compounds containing main group atoms,[87] organic chemical reactions as short-lived intermediates,[88b,95] thermal sigmatropic migrations such as the Cope rearrangement,[96] optical transformations[97] and in dye-sensitized solar cells within singlet fission chromophores.[98] In order to know the exact amount of singlet diradical character in the wave functions of different chemical systems, it is important to be able to quantify it. However, there are no direct means to experimentally measure singlet diradical character since it is not a physical observable but a property of the wave function.[99] Nevertheless, an indirect indication of singlet diradical character of a molecular system can be obtained by measuring the energy difference between its lowest singlet and triplet states. A small singlet-triplet gap generally corresponds to strong singlet diradical character and the inverse is true as well. However, there exists one problem in quantifying singlet diradical character through the singlet-triplet gap: a zero splitting between the lowest singlet and triplet states naturally corresponds to a pure (100%) diradical, but no clear-cut definition for 0% diradical character can be made. Another method to quantify singlet diradical character from experimental data employs the valence configuration interaction scheme in which the necessary quantities are taken from one- and two-photon absorption spectra, phosphorescence and electron spin resonance peaks.[100] It was, however, noted that the values determined through this route deviate from theoretical data

without scaling. Hence, the quantification of singlet diradical character is still strongly based on theoretical methods.

From a theoretical point of view, singlet diradical character can be qualitatively determined from the calculated singlet-triplet gaps and from the forms of magnetic orbitals obtained via broken symmetry calculations.[101a] As in the case of experimental characterization methods, these analyses are not capable of quantifying the extent of singlet diradical character in any precise manner. Thus, a variety of different methods have been developed which are able to give an accurate numeric description of singlet diradical character. For example, the quantification of singlet diradical character in these methods is based on second hyperpolarizabilities,[102] the magnitude of spin contamination in the broken symmetry determinant,[101] natural orbital occupation numbers obtained from general valence bond calculations[103] and on orbital overlap.[104] In addition to the above methods, multiconfigurational approaches can also be used to determine the amount of singlet diradical character either from the CI vector coefficients[105] or from the natural orbital occupation numbers (NOONs).[106]

Because the wave functions of singlet diradicals are multiconfigurational, their description requires at least two Slater determinants whose weights are determined by the CI vector coefficients. In a perfect singlet diradical, the Hartree-Fock determinant and the doubly excited determinant have equal weights in the multiconfigurational wave function, in which case the corresponding CI vector coefficients C_{RHF} and C_{DE} are both $2^{-½}$.[xvi] The diradical character can then be defined with a simple relation

$$\frac{(C_{DE})^2}{(2^{-½})^2} \times 100\% = 2(C_{DE})^2 \times 100\% \qquad (3.6)$$

which approaches unity (100 %) for pure diradicals and zero (0%) for closed shell singlet states.[105]

Alternatively, NOONs from a multiconfigurational wave function can be used to evaluate the amount of singlet diradical character.[106] The natural orbitals are those which diagonalize the one-particle density matrix, and their occupation numbers are the eigenvalues of this matrix.[107] In a perfect diradical, the two natural orbitals which are associated with the diradical character have identical occupation of one electron each.[106] However, occupation numbers deviate from one in all imperfect diradicals and an index for singlet diradical character can be obtained by comparing the occupation number of the acceptor orbital (n_{ACC}) to the reference value of one electron

$$\frac{n_{ACC}}{1} \times 100\%. \qquad (3.7)$$

It has been shown that as the level of theory increases, NOONs converge towards values that they adopt in the exact wave function.[108] However, as the

[xvi] This can be easily seen from Equation 3.5 in which C_1 and C_2 correspond to the C_{RHF} and C_{DE} CI vector coefficients, respectively.

exact wave function cannot be reached for many electron systems, the accuracy of the NO analysis depends on the quality of the multiconfigurational wave function used in the actual calculations. This holds also when using the CI vector coefficients in the analysis. Hence, if the multiconfigurational wave function is based on only two determinants, which is the minimum active space in calculations of singlet diradicals, the amount of singlet diradical character becomes overestimated by both methods.[23,93] In order to obtain close to converged results, it is recommended that an active space close to the full valence space is used. In case of NOONs, occupations calculated at the CISD(T) and CCSD(T) levels of theory can also be used if the system of interest has only a small or moderate amount of diradical character in its wave function.[108] It should also be noted that the NO analysis always predicts slightly higher diradical character than the CI method as the acceptor orbitals contain also electron density from excitations other than that associated with the diradical nature.

3.2 Quantum chemical methods for the calculation of static electron correlation effects

As explained above, multiconfigurational character arises from the fact that wave functions are dominated by more than one Slater determinant and it is static electron correlation, not dynamic, that is needed to model these (near) degeneracy effects. However, in quantum chemistry, the distinction between dynamic and static electron correlation is sometimes wavering as both correlation effects are simultaneously present at the wave function.[23,93] Thus, in many calculations, quantum chemical methods which take into account both dynamic and static correlation effects must be used. An alternative to multiconfigurational approaches is offered by the broken symmetry formalism which is significantly less accurate in modeling static electron correlation but applicable to much larger systems.[109]

3.2.1 Broken symmetry formalism

The HF model, be it restricted or unrestricted, is an inadequate approximation of a multiconfigurational wave function. Hence, in many cases, it is often necessary to test the applicability of the HF model to a given problem by testing the stability of the self-consistent field (SCF) solution with respect to different constraints.[23] Negative eigenvalues in the stability analysis indicate instability in the wave function which means that a lower energy solution can be obtained by allowing more flexibility to the wave function. Typically the instability of an SCF solution is a sign of multiconfigurational character in the wave function and the restricted-unrestricted instability in particular often indicates the presence of singlet diradical character.

In contrast to RHF, the unrestricted Hartree-Fock (UHF) method allows an open shell wave function whose spatial symmetry can relax. It is exactly this

flexibility of the UHF wave function that is used in unrestricted broken symmetry formalism to simulate static electron correlation effects by allowing α and β MOs to localize on different atomic centers.[109] In case of singlet diradicals this means that two electrons with antiparallel spins can occupy two spatially different MOs even though the multiplicity of the total wave function is still formally a singlet.[94b,109] However, there is one serious drawback in this formalism: the UHF wave function for a singlet state is not a pure spin state but a spin contaminated mixture of singlet and triplet states. This means that the wave function is not anymore an eigenfunction of the total spin operator. Hence, the broken symmetry approach should not be used for accurate quantitative analysis although the eigenvalue of the total spin operator has been employed to quantify the amount of singlet diradical character.[101]

Similarly to the RHF wave function, the stability analysis can also be performed for a restricted Kohn-Sham SCF solution.[34] However, the absence of negative eigenvalues in this case does not always exclude instability in the wave function though the opposite is always true. This is due to the fact that in the DFT formalism, instability reflects the capability of the chosen exchange-correlation functional to describe the electron density with a single Slater determinant constructed from Kohn-Sham orbitals, whereas in the HF formalism the instability serves as a direct measurement of the quality of the wave function. In principle, DFT should give a proper description of molecular systems with multiconfigurational character in their wave function even without the need to use broken symmetry formalism. Unfortunately, this only holds if the exact exchange-correlation functional is known. As all practical calculations use approximate exchange-correlation functionals, they have the same shortcomings as all other single determinant-based methods. However, there are a couple of exceptions when broken symmetry DFT calculations perform well for singlet diradicals. If the two partially occupied MOs Φ_a and Φ_b are disjoint, the broken symmetry DFT approach typically gives reasonable results.[110] In addition, if the singlet diradical character is small or moderate, exchange-correlation functionals without exact (HF) exchange generally outperform their hybrid variants in calculations.[34]

3.2.2 Multiconfigurational methods

Multiconfigurational methods give a very balanced description of wave functions that are dominated by static electron correlation effects.[23,93] The most commonly used method to treat static electron correlation is the multiconfigurational self-consistent field (MCSCF) approach in which the shortcomings of single determinant-based methods are avoided by variationally optimizing the orbitals together with the CI coefficients of several electronic configurations. However, the simultaneous optimization of orbitals and CI vector coefficients is a difficult nonlinear problem, which strictly restricts the length of MCSCF expansions. This introduces the most important challenge in MCSCF calculations: the selection of an appropriate configuration space. In early applications of the MCSCF formalism, configurations were selected individually based on physical

and chemical insight, but nowadays the partitioning of orbital space is done in a more systematic manner. Two of the most commonly used variants of the MCSCF approach are the complete active space (CAS)[111] and the restricted active space (RAS) methods.[112]

In CAS calculations, the orbital space is divided into three different sets of orbitals that are the inactive (core), active and secondary (virtual) orbitals.[23,93] The inactive and secondary orbitals are doubly occupied and unoccupied, respectively, in all configurations. In contrast, there are no limitations to the occupancies of the active orbitals. Hence, the CAS wave function contains all configurations which can be generated by doing a FCI within the active space. In this respect, a CAS wave function takes into account all electron correlation effects within a limited orbital subspace.

In RAS calculations, the active space is further partitioned into three subspaces which are called RAS1, RAS2 and RAS3.[23,93] The RAS2 space is exactly the same as the CAS active space and is therefore not subjected to restrictions in electronic excitations. However, the RAS1 and RAS3 spaces set more restrictions to the allowed excitations. The RAS1 space consists of formally doubly occupied orbitals in which a certain number of holes can be allowed. For example, only single and double excitations can be done from of these orbitals. In contrast, the RAS3 space can be occupied with only a given number of electrons in different configurations, that is, only certain electron excitations are allowed to these formally unoccupied orbitals.

Although CAS and RAS methods are extremely powerful tools in computational quantum chemistry and make it easier to carry out MCSCF calculations, they are far away from being black box methods.[23,93] Choosing the active space is a complex task that requires much physical insight to the problem at hand. The easiest way to ensure that a balanced description of a system is obtained is to include all valence electrons and orbitals into the active space. However, this is only possible for the smallest of systems since the number of configurations becomes unmanageably large as the size of the active space increases. Nowadays, the maximum amount of active orbitals is between 10 and 20, which means that the choice of the active space must be done very carefully. Localized or natural orbitals from high-level single determinant methods can be used as guidelines in this process, but it has to be remembered that, in extreme cases, they might have only little or no relevance to the actual multiconfigurational character of the system in question.

An MCSCF wave function offers the best way to treat (near) degeneracy effects, but it has reduced capabilities to describe dynamic electron correlation due to limitations in the size of the active space.[23,93] For quantitative accuracy, dynamic electron correlation can be taken into account via MPPT, CI or CC approaches. Two of the most widely used methods are CAS augmented with second order perturbation theory (CASPT2)[113] and multireference configuration interaction (MRCI).[114] In recent years, a lot of development has also been done on methods in which the MCSCF wave function is augmented with a coupled cluster-based ansatz.[115] Both CASPT2 and MRCI produce very balanced wave

functions and they can be used to model exceptionally complex systems. Unfortunately, they suffer from the same problems as their corresponding single determinant variants. Specifically, CASPT2 gives non-variational energies and MRCI is not size-consistent.[23,93] The size-consistency problem of MRCI can, however, be easily corrected by introducing a correction for quadruple excitations in an *ad hoc* manner, which gives the MRCI+Q approach.[116,xvii]

3.3 Results and discussion

3.3.1 Chalcogen-nitrogen heterocycles Ch_4N_4 (Ch = S or Se)

Weak transannular chalcogen···chalcogen (Ch···Ch) interactions are a recurring theme in the chemistry of certain electron-rich inorganic ring systems.[117] Probably the most well-known example is tetrasulfur tetranitride, S_4N_4 (**10a**), which is structurally related to the eight membered homopolyatomic chalcogen dications (see Section 2.2.2).[79h] However, the presence of two fewer valence electrons in **10a** compared to **7** gives it a cage-like structure with not just one but two short transannular S···S interactions that are significantly elongated if compared to a typical S-S single bond (Figure 7).[79c,e,g] The selenium analogue (**10b**)[79b,d,f] of S_4N_4 as well as the hybrid species $Se_2Se_2N_4$ (**10c**)[79a] can also be synthesized and they are both structurally isomorphous to S_4N_4 with two transannular Ch···Ch contacts.

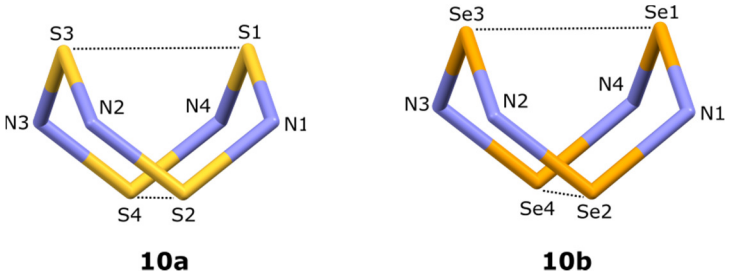

Figure 7. The cage-like molecular structures of S_4N_4 (**10a**) and Se_4N_4 (**10b**) with two weak cross-ring Ch···Ch interactions. Average experimental bond lengths: r[S1···S3] = r[S2···S4] = 2.596(1) Å and r[Se1···Se3] = r[Se2···Se4] = 2.742(2) Å.[79c,79d]

Although a qualitative picture of the relevant bonding interactions in **10** can easily be derived from the basic cluster framework, cuneane, by following Gillespie's structural rules,[76b] the exact nature of the short Ch···Ch contacts in **10** has initiated much debate ever since the crystal structure of **10a** was first reported.[77] Over the years, the weak bonding interactions in **10** have been probed using extended Hückel calculations as well as more advanced quantum chemical methods such as HF, DFT and MP2. Unfortunately, it has proven very diffi-

[xvii] The quadruple correction has several different variants. For further details, see reference 116a and references therein.

cult to accurately predict the molecular geometry of **10** using computational approaches. For example, the Hückel approximation[77k] indicates that **10a** should display a classical σ-bonded structure instead of weak Ch···Ch interactions and this picture is retained at the HF level.[77e] If the transannular interactions in **10** are primarily orbital-based (covalent) as suggested by both Hückel and HF data, dynamic electron correlation effects should have only a minimal effect on the calculated geometries. However, the use of perturbation theory leads to significant overestimation of the Ch···Ch interactions even when increasing the order of perturbation up to the fourth order.[77b] DFT also has severe difficulties in reproducing the experimental geometries of **10** and the performance of the B3LYP hybrid functional is notoriously poor as it significantly overestimates (up to 1Å) the Ch···Ch contacts.[77b]

Because a solid physical explanation of transannular interactions in heterocyclic chalcogen rings **10** was still lacking and these interactions had gained renewed interest,[118] a detailed theoretical study of bonding in **10a** and **10b** was conducted at the highest possible levels of theory. The following is a short summary of the original results reported in full in research Paper **II**.

The geometries of heterocyclic rings **10a** and **10b** were first optimized using single determinant-based methods including HF, MPPT, QCISD(T), CCSD(T) and DFT. All aforementioned levels of theory predicted Ch-N bond lengths which were very close to the experimental values, but the optimized transannular Ch···Ch distances varied much more between different methods (Figure 8). At the HF level, the Ch···Ch contacts were slightly underestimated, while the performance of the perturbation series depended on the order of the perturbation. Both MP2 and MP4 overestimated the Ch···Ch interactions, whereas the results at the MP3 level were in reasonable agreement with the experimental data. The overall performance of the MPPT series clearly demonstrates that the Ch···Ch interactions cannot originate purely from closed shell interactions as these are already accounted for (at least semi-quantitatively) at the MP2 level.[27,82] The QCISD(T) and CCSD(T) methods were the only single determinant *ab initio* approaches which were able to predict the Ch···Ch distances in tetrachalcogen tetranitrides in good agreement with the experimental data.

Interestingly, the DFT methods (particularly BLYP) performed better for Ch_4N_4 than for Ch_8^{2+} even though a similar trend between the amount of exact exchange and the transannular Ch···Ch distance was observed in both cases. Furthermore, the PBE0 functional showed again the best performance and the effect of empirical dispersion correction (DFT-D3) was only minute.

The crystal structures of **10a** and **10b** contain several intramolecular interactions that could have a strong impact on the observed geometries.[79] If the observed transannular distances are long simply due to crystal packing effects and secondary bonding interactions, the comparison of calculated gas phase geometries to the X-ray data is not justified. However, the gas-phase electron diffraction study of **10a** is consistent with the X-ray data[119] and the solid-state calculations for S_4N_4 at the HF, B3LYP, PBE and PBE0 levels of theory converge to sim-

ilar geometries as the gas phase optimizations. Thus, these findings support the fact that secondary bonding interactions do not play an important role in determining the transannular distances, thereby validating comparisons between gas-phase and X-ray data.

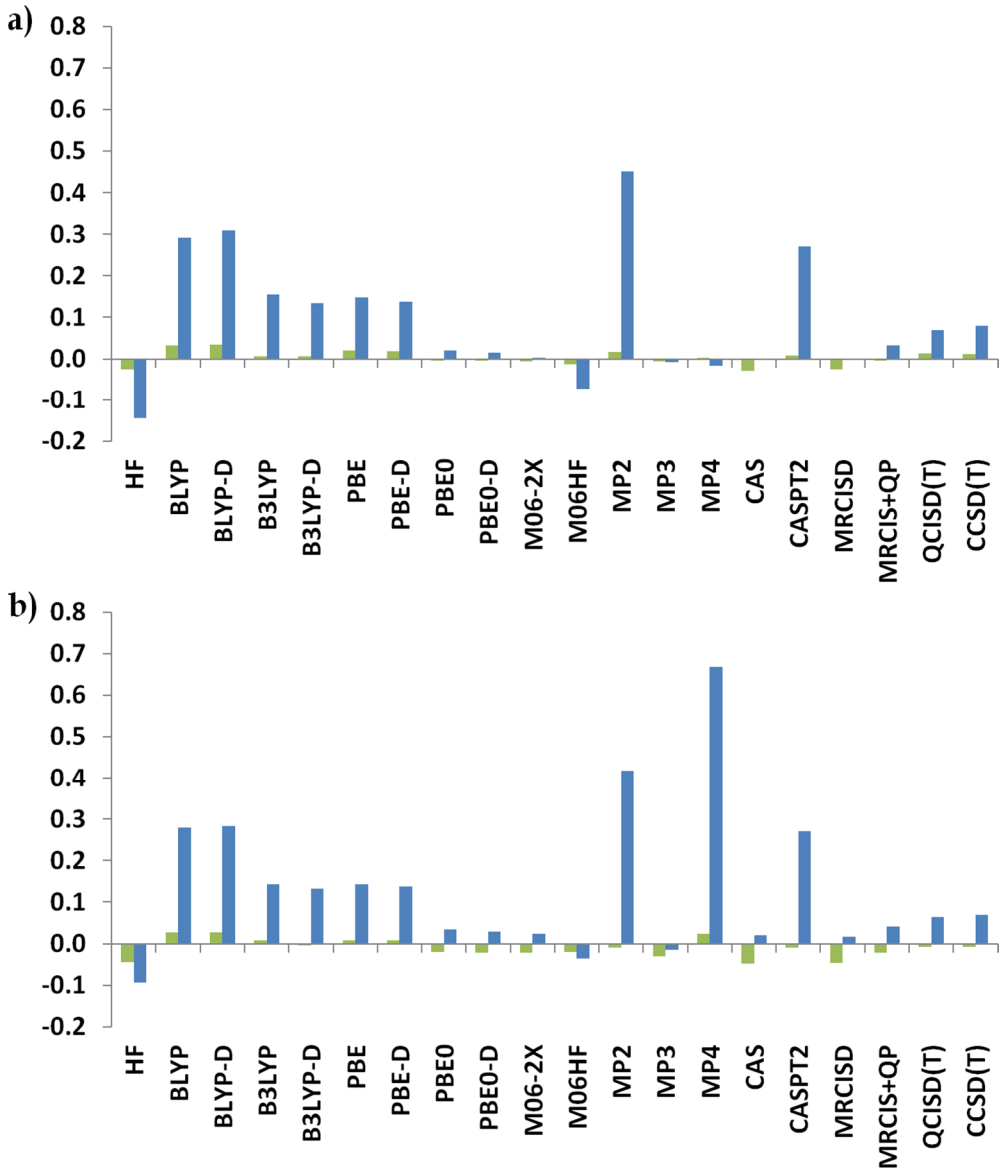

Figure 8. Deviations between the calculated and experimental bond lengths [Å] for (a) S_4N_4 and (b) Se_4N_4.[79d,119] All data calculated in the gas phase. Color code: Ch-N bond lengths (green), Ch···Ch (blue).

Before the wave functions of Ch_4N_4 were modeled using multiconfigurational methods (CAS, CASPT2, MRCI and MRCI+Q), a natural orbital analysis was performed for the optimized geometries at the QCISD(T) level of theory. The NO analysis revealed that both **10a** and **10b** had a number of NOs whose occupation numbers deviate significantly from 2 or 0. Typically NOONs that are less than 0.05 e^- are observed for molecular systems that are well-described by a single Slater determinant. Hence, the results of NO analyses indicated that

the electronic structures of Ch_4N_4 are influenced by strong electron correlation effects. The most important fractionally occupied NOs were found to be associated with the Ch···Ch interactions: two bonding orbitals having NOONs of 1.88 e^- each and two antibonding orbitals with NOONs of 0.16 e^- each (Figure 9). Thus, these were the four most important orbitals to be included in the active space in subsequent multiconfigurational calculations.

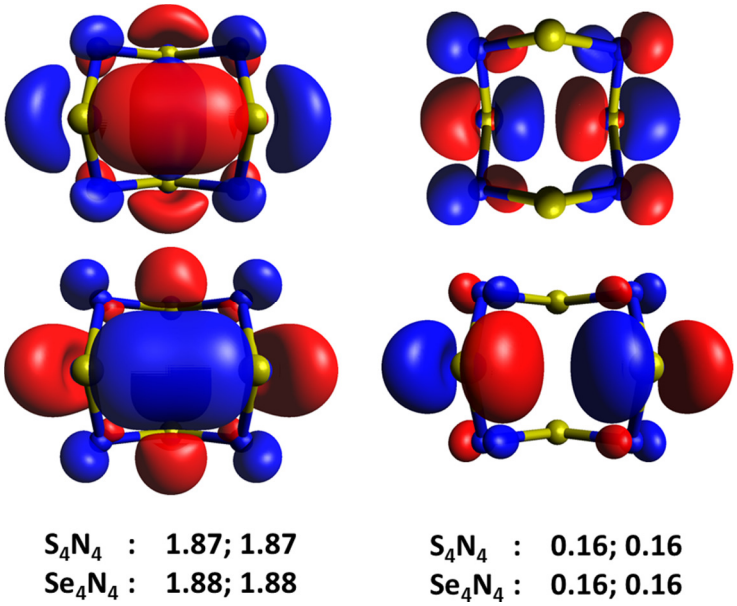

Figure 9. The most important fractionally occupied QCISD(T) natural orbitals of E_4N_4 along with their occupancies.

In contrast to the Ch_8^{2+} dications, the geometries of tetrachalcogen tetranitrides, and the Ch···Ch interaction in particular, were found to be well-described at the CAS level of theory. The inclusion of dynamic electron correlation effects via MRCI improved the results only slightly. This was strong evidence that static, not dynamic, electron correlation plays an important role in the wave functions of Ch_4N_4. A more detailed analysis of the CI vector coefficients revealed that the wave functions of Ch_4N_4 indeed contain diradical character, as well as tetraradical character, associated to each Ch···Ch interaction. These results were further supported by UHF calculations that predicted the triplet and quintet states of Ch_4N_4 to be lower in energy than the singlet state. A rough estimate of the singlet diradical character in Ch_4N_4 was obtained from the NOONs and it was found to be approximately 10 % per Ch···Ch bond.

At this point it was yet unclear why the CASPT2 method, although being able to take into account static electron correlation, significantly overestimates the Ch···Ch contacts in both tetrachalcogen tetranitrides. The poor performance of the perturbation correction was ultimately traced to the overestimation of the role of doubly excited determinants in the total wave function. It also needs to be noted here that since the wave functions of Ch_4N_4 contain important static electron correlation effects, it was not entirely surprising that the different density functionals performed much better than in the case of Ch_8^{2+} dications.

In light of all of the above data, it could be concluded that the transannular interactions in Ch_4N_4 originate from covalent bonding which becomes significantly elongated and weakened primarily due to static electron correlation effects. Thus, only a small number of excited determinants are needed to obtain an accurate description of their electronic structures. In this respect, the diradical character associated with the Ch···Ch interactions in Ch_4N_4 is reminiscent of weak exchange-coupling of two radical species via overlap of their singly occupied molecular orbitals.

3.3.2 REER dimetallenes (E = Al-In; R = alkyl, aryl)

Although it was long thought that the electron deficient nature of group 13 elements prevents the formation of homonuclear multiple bonds, Berndt and Klusik ultimately showed that compounds containing B=B bonds could be synthesized via reduction of tetraorganodiboron species.[120] Shortly after these findings, the heavier monoanion radicals $[R_2EER_2]^{\bullet-}$ (E = Al or Ga), with a formal π-bond order of one-half, were also reported.[121] Solid state structural studies confirmed that these radicals have shorter E-E bond lengths than the neutral species R_2EER_2, which is consistent with the formation of a π-type interaction.

The true revolutionizing step in the chemistry of group 13 homonuclear multiple bonds was the report of Robinson *et al.* on the digallyne salt $Na_2[RGaGaR]$ (R = C_6H_3-2,6-(C_6H_2-2,4,6-$^iPr_3$)$_2$) in 1997 as it was the first heavier group 13 alkyne analogue.[122] However, the observed Ga-Ga bond length (2.32 Å) was not much shorter than a typical Ga-Ga single bond (2.48 Å) and the -CGaGaC- array had a markedly trans-bent structure with bridging Na^+ ions. This initiated a lively debate regarding the nature of the Ga-Ga bond in this compound and various theoretical approaches were used to examine its electronic structure.[5,7] Because different theoretical studies gave different descriptions of the nature of bonding in $Na_2[RGaGaR]$, a solution to the problem was sought through synthesis of the neutral RGaGaR species that should contain a Ga=Ga double bond.

The structure of the first neutral digallene RGaGaR (R = C_6H_3-2,6-(C_6H_3-2,6-$^iPr_2$)$_2$) was published by Power *et al*. five years after the digallyne salt and it was found to have a similar trans-bent geometry with a long Ga-Ga bond (2.63 Å).[123] In addition, cryoscopic measurements suggested that the dimer dissociates to RGa: monomers in solution, especially when bulky substituents were used.[124] Hence, experimental data indicated that the Ga-Ga "double" bond in RGaGaR was considerably weaker than a single bond, which also cast doubt on the existence of a Ga-Ga triple bond in the digallyne salt. Shortly after, the heavier In and Tl analogues of RGaGaR were also synthesized and they were shown to adopt similar trans-bent structures in the solid state.[85,125] However, all attempts to synthesize corresponding dialuminenes gave only the cycloaddition product of the putative dimetallene with the solvent, indicating different reactivity for these species.[126]

A number of different theoretical studies have been published with the focus on explaining the nature of bonding in the formally doubly bonded dimet-

allenes.[5a,b,6a,7b,c,f,8,9] At first, an explanation of the structures of dimetallenes was given based on a donor-acceptor bonding model,[6a,8] but later studies have concentrated on the role of the "slipped" π-type orbital in the bonding description. This orbital is the HOMO of dimetallenes and it is formally antibonding with respect to the metal-metal bond.[5a,b] If the most important bonding interactions in dimetallenes truly originate from the "slipped" π-type orbital, then the HF method should predict their molecular geometries in reasonable agreement with experimental data. However, HF calculations yielded structures with Ga-Ga bonds that are weaker and significantly elongated compared to the experimental bond lengths.[5a,b,6a] In contrast, DFT calculations yielded accurate geometrical parameters for digallenes, but the Ga-Ga interactions were nevertheless predicted to be very weak and similar in strength to closed shell interactions.[9] However, it is not entirely clear how the standard formalism of DFT is able to describe bonding in dimetallenes since it does not take into account dispersion effects.

As neither orbital nor closed shell interactions alone seem to offer a solid physical explanation of bonding in dimetallenes, a detailed theoretical investigation of the electronic structures of model systems **11-13** was performed. The results of this study are presented in full in research Paper **III** and a short review of the most important findings is given below.

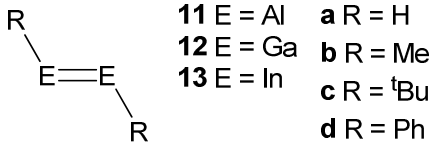

The geometries of **11-13** were first optimized with three standard quantum chemical methods: HF, MP2 and B3LYP (Table 3). As seen from the results, only MP2 and B3LYP gave bond lengths which were in reasonable agreement with the experimental values. By testing the stabilities of the RHF wave functions it was found that all of the model systems had restricted-unrestricted instabilities and lower energy solutions could be obtained by using the broken symmetry approach. The resulting UHF optimized structures were approximately 5-20 kJ mol^{-1} lower in energy than the corresponding RHF solutions and in much better agreement with the experimental data (Table 3), which indicated that all of the lighter dimetallenes **11-13** have a small amount of singlet diradical character in their wave functions. The presence of singlet diradical character in **11-13** is not entirely unexpected considering that the analogous diboronenes have triplet ground states.[127]

Table 3. Optimized metal-metal bond lenghts [Å] in **11-13** at different levels of theory.

	HF	UHF	MP2	CCSD(T)	CAS	CASPT2	B3LYP	Exptl.
11a	2.78	2.57	2.65	2.65	2.68	2.62	2.67	
11b	2.91	2.73	2.72	2.71	2.75	2.66	2.74	
11c	2.95	2.64	2.71	-	2.78	-	2.76	
11d	2.91	2.70	2.69	-	2.73	-	2.73	
12a	2.79	2.65	2.55	2.57	2.66	2.50	2.64	
12b	2.92	2.70	2.61	2.62	2.72	2.53	2.70	2.51-
12c	2.96	2.74	2.60	-	2.75	-	2.71	2.63[a,b]
12d	2.95	2.95	2.59	-	2.70	-	2.69	
13a	3.34	3.33	2.97	2.99	3.10	2.88	3.06	
13b	3.45	3.12	3.02	3.04	3.16	2.92	3.11	2.98[c]
13c	3.50	3.13	3.00	-	3.20		3.13	
13d	3.73	3.70	3.01	-	3.18	-	3.14	

[a]Reference 124. [b]Reference 123. [c]Reference 125.

A proper treatment of diradical character in dimetallenes requires the use of a wave function which has (at least) two configurations: in addition to the RHF determinant, the configuration which transfers electrons from the E-E antibonding HOMO to the E-E bonding LUMO+1 is needed. Pictorially this correlation can be represented by drawing the Lewis structures **A** and **A'** which correspond to the RHF and doubly excited determinants, respectively (Figure 10). When such static electron correlation is included in the calculations via a CAS wave function, the geometries of dimetallenes are found to be in much better agreement than HF with the experimental data. The agreement can be improved even more if dynamic electron correlation is included via perturbation theory (CASPT2). This is particularly true for diindenes, which serves as a good illustration of the fact that closed shell interactions become stronger as the atoms become heavier. In this respect, it needs to be noted that the electronic structures of dithallenes were found to be exclusively governed by dynamic electron correlation effects (see Section 2.2.3).

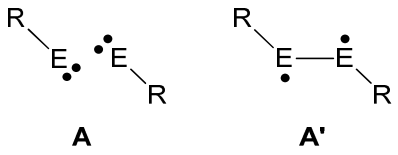

Figure 10. Lewis structures describing the RHF (**A**) and the doubly excited singlet diradical determinant (**A'**) of dimetallenes.

The amount of singlet diradical character in dimetallenes was quantified using both CI vector coefficients and NOONs, and found to be the strongest in dialuminenes (15%) and the weakest in diindenes (6%). Consequently, the diradical character in **11-13** ranges from small to moderate, which readily explains the good performance of both DFT and CCSD(T) in geometry optimizations (Table 3). However, the calculated data at the MP2 level is surprisingly

accurate which is somewhat unexpected. A subsequent analysis of natural orbitals and their occupation numbers revealed that the good performance of the MP2 method was fortuitous and resulted mainly from the overestimation of closed shell interactions at this particular level of theory.

Table 4. Interaction energies [kJ mol^{-1}] of **11-13**.

	HF	UHF	B3LYP	CCSD(T)
11a	-25	-40	-63	-64
11b	-15	-46	-47	-50
11c	-11	-25	-45	
11d	-12	-19	-47	
12a	-17	-35	-52	-51
12b	-11	-25	-41	-41
12c	-9	-11	-41	
12d	-8	-8	-39	
13a	-8	-8	-31	-30
13b	-7	-11	-28	-24
13c	-6	-11	-29	
13d	-3	-3	-23	

To gain more insight into the strength of E-E bonds in dimetallenes, the interaction energies of **11-13** were calculated at different levels of theory (Table 4). All methods gave the same qualitative trend: when the size of the group 13 element increases, the strength of the E-E bond decreases. Moreover, energy analysis at the HF level undoubtedly proved that the "slipped" π-type orbital interaction makes only a small contribution to the bonding of all systems studied. The use of an UHF wave function gave slightly better interaction energies for all systems, but to further quantify the strength of the metal-metal interaction in **11-13**, the interaction energies were also calculated by using the theoretically most accurate the CCSD(T) and B3LYP approaches. At these levels of theory, the interaction energies of **11-13** were approximately between -60 and -25 kJ mol^{-1}; these absolute values are much smaller than the typical single bond energies (Al, 219 kJ mol^{-1}; Ga, 242 kJ mol^{-1}; In, 203 kJ mol^{-1}) calculated for reference systems $H_2E\text{-}EH_2$.[xviii] These data lend strong support to the view that the E-E bonding in group 13 dimetallenes is by all standards considerably weaker than in a typical single bond.

[xviii] The single bond energies were evaluated by calculating the dissociation energies of E-E bonds in $H_2E\text{-}EH_2$.

4 SPIROCYCLIC MAIN GROUP RADICALS

A number of experimental and theoretical studies have shown that, in addition to metals and inorganic semiconductors, free radicals can be used to manufacture conducting and magnetic materials.[128] However, in order for a molecular radical-based material to behave like a bulk metal it needs to fulfill two criteria.[129] First, its building blocks, the neutral molecular radicals, should have long enough lifetimes. Second, these molecules should arrange themselves in the solid state in a manner that enables the transmission of magnetic or conductive interactions in three dimensions. Because of these prerequisites, chemists have in recent years put much effort on the rational design of new stable radicals.[128,130,131] The study of radical species is also important from a purely fundamental perspective as it helps to develop our understanding of molecular structure and bonding.

Being mostly organic, free radical magnets and conductors would have one significant advantage over traditional metals and inorganic semiconductors: they would be modifiable through chemical synthesis. Since both metals and semiconductors have an indispensable function in the modern technological society, it is not difficult to imagine what the impact of molecular materials with analogous properties would be. However, a lot of work still remains to be done in this research area as metal-like room temperature free radical conductors still await their discovery. Furthermore, all currently known molecular radicals that achieve magnetic ordering in the solid state do so only at extremely low temperatures.[132] Consequently, the quest for new stable radicals with properties more tuned for the synthesis of molecular metals continues vigorously.

The following two subchapters begin with an introduction to techniques used in the stabilization of molecular radicals. Specific emphasis is put on spiroconjugation, which is then discussed in the context of neutral coordination compounds of stable main group radicals with group 13 elements. The results and discussion part reports a specific case study under the same topic whose results were originally published in the research Paper **IV**.

4.1 Stabilization of radical species

Long-lived radicals are usually divided into two categories: stable and persistent radicals.[xix,131,133] The first group includes radicals which can be isolated and handled as pure compounds under an inert atmosphere at room temperature, whereas the second group contains radicals which are sufficiently long lived to be observed by spectroscopic methods.[131] As can be easily imagined, the synthesis of stable radicals is not a straightforward task due to the intrinsic nature of unpaired electrons to pair up, *i.e.*, to form chemical bonds. For this reason, different methods are being employed to stabilize free radicals. Two of the most common approaches involve steric protection of the radical site (kinetic stabilization) and extensive delocalization of the unpaired electron within a π-type system.

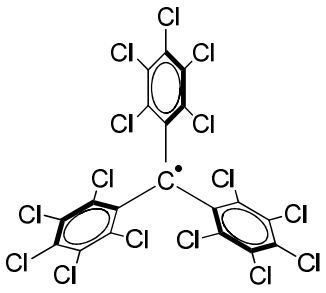

14

The best and most well-known example of a sterically (and to some extent delocalization) stabilized radical is the polychlorinated triarylmethyl (PTM) radical **14** in which the unpaired electron resides on a methyl carbon that is entirely protected by three fully chlorinated phenyl rings.[134] The most important for the protection are the chlorine atoms in *ortho*-positions, whereas the halogens in *para*-positions can be removed and changed for different groups or atoms without suppressing the stability of the radical.[129] This architecture makes the PTM radical extremely stable and, consequently, its lifetime is measured in decades under ambient conditions. Thus, PTM is called an inert carbon-free radical and it behaves very much like a classical organic compound. Unfortunately, the strong kinetic stabilization of the radical site in PTM suppresses both unwanted and wanted reactivity, and some of the synthesized PTM derivatives are remarkably inert to almost all reagents and do not even undergo normal radical combination reactions.[129,135] Moreover, steric hindrance also prevents spin interactions between radicals that is essential, for example, for establishing magnetic coupling.

A second popular method to stabilize radicals is to use extensive delocalization of the unpaired electron.[130,131] The phenalenyl ring (**15**) is an archetypical example of a radical stabilized through this route.[136] Although the unpaired

[xix] The definition of stable and persistent radicals is somewhat dependent on the author. See references 131 and 133 for further details.

electron is delocalized by the conjugated π-system, the parent radical exists in equilibrium with the σ-dimer (**15′**) in solution. The phenalenyl radical also shows sensitivity towards oxygen which is itself a stable triplet radical. However, in deoxygenated and dilute solutions, the phenalenyl radical has a long lifetime even without further steric protection, which illustrates the effectiveness of electron delocalization in radical stabilization. If further stability of the molecular framework is sought, it can be obtained by introducing more steric bulk to the carbon-based backbone in phenalenyls, which prevents the formation of a σ-dimer.[137] Indeed, the placement of three ^{t}Bu groups at the three peripheral carbons completely inhibits the σ-dimerization pathway and leads to π-stacking of the phenalenyl radicals in the solid state (**15′′**). This gives rise to antiferromagnetically coupled π-dimers which are indefinitely stable in the solid state under an inert atmosphere. However, the steric protection by ^{t}Bu groups does not prevent **15′′** from reacting with oxygen, which means that under ambient conditions, the dimer readily decomposes to phenalenone derivatives (as well as to other unidentified products) within one week.

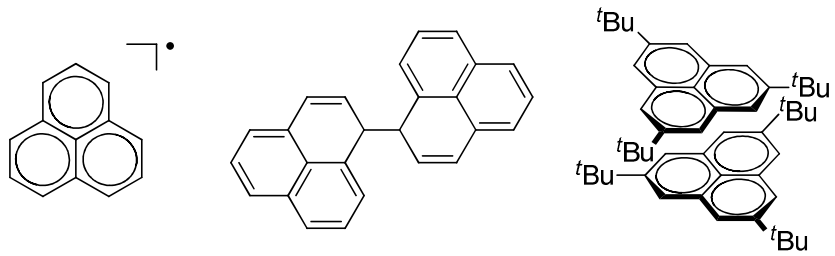

15 **15′** **15′′**

Even though the PTM and phenalenyl radicals are among the most widely known examples of stable radicals, they are by no means the only systems that can be stabilized through steric protection or electron delocalization. For example, kinetic stabilization has been used to stabilize cyclopentadienyl[138] and aminyl radicals,[139] the isolation of the latter requiring the use of extreme steric bulk. In principle, any π-type radical offers the possibility to delocalize spin density over its π-system, though cyclic molecules are better than acylic ones since they maximize conjugation.[130] Some respective examples of radicals exhibiting π-delocalization are Gomberg's triphenylmethyl radical[140] as well as sulfur-nitrogen-based heterocyclic radicals such as thiazyls.[141] Another more specific way to increase the stability of radicals via delocalization of the unpaired electron is to use spiroconjugation.[142]

4.1.1 Spiroconjugation

A spirocyclic coordination compound has a structure in which two ligands are in a mutually perpendicular orientation and coordinated to a central element.[142] If both ligands have an antisymmetric π-type frontier orbital, their perpendicular orientation maximizes the orbital overlap, which gives rise to spiroconjuga-

tive interactions over the central element and, consequently, to splitting of the energy levels (Figure 11, left). In spiroconjugated radicals, the conjugated orbitals are only partially occupied, which means that the unpaired electron is delocalized over the entire molecular framework, greatly increasing the stability of the radical. If, on the other hand, the two ligands have symmetric π-type orbitals, a spirocyclic structure is formed but the orbitals cannot interact with each other and remain essentially degenerate (Figure 11, right).

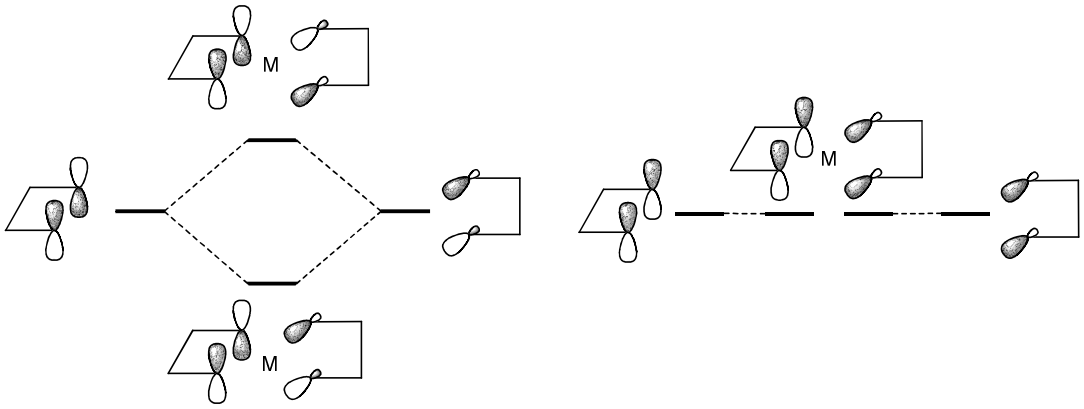

Figure 11. In spirocyclic systems, conjugative orbital interactions over the central insulating element (M) lead to the splitting of the energy levels (left), whereas non-conjugative interactions give rise to a degenerate orbital set (right).

Spiroconjugation is a recurring theme in the field of molecular materials science since it offers an excellent framework to stabilize radicals.[143,144,145] This unique molecular framework has been used in different purposes, for example, to stabilize chelating main group ligands with atypical charges,[145] to investigate intermolecular spin transfer[144b] and to create stable triplet state diradicals.[144c] The extensive delocalization of the unpaired electron in spiroconjugated structures also resolves two problems that are related to the synthesis of neutral radical conductors.[146] The first is Peierls instability which, at the molecular level, means that radicals typically associate into closed shell dimers, leading to either a semiconducting or purely insulating ground state. The second is the trapping (localization) of the spins on radical sites which suppresses charge transportation. Moreover, the small frontier orbital level splitting in spiroconjugated radicals gives rise to an unconventional quarter-filled energy band in the solid state, which increases the conductivities of these radicals much more than could be achieved by delocalization alone.[143d] In light of these data, it can be concluded that the spiroconjugated structural motif is an excellent molecular framework to create neutral radicals with potential applicability in the field of molecule-based materials.

4.2 Stable neutral spirocyclic radicals involving group 13 elements

Spirocyclic bis-phenalenyls (**16**-**18**; R = alkyl, aryl) are one of the most well-known stable spiroconjugated radicals.[143] These molecules have interesting magnetic, conductive and electrochemical properties and they can be easily synthesized by reduction of their corresponding cationic salts with a common reducing agents such as cobaltocene, tetrakis(dimethylamino)ethylene or bis(pentamethylcyclopentadienyl)-nickel(II).

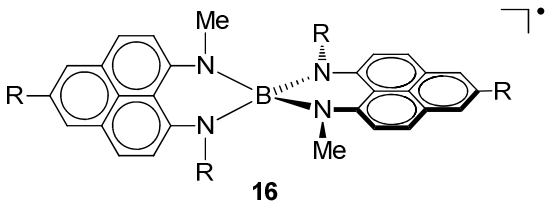

16

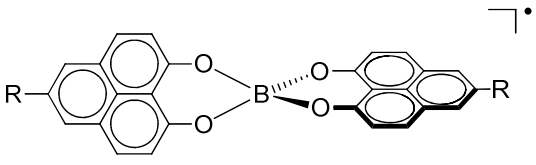

17

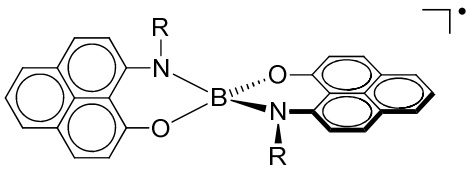

18

All spirocyclic bis-phenalenyl radicals have a similar spiroconjugated structure in which two perpendicular phenalenyl rings with antisymmetric π-type frontier orbitals are held together by a single boron atom.[143] The solid state packing of spiro-bis-phenalenyls has been intensively studied by Haddon *et al*. using X-ray diffraction. Their results have revealed that the spiro-bis-phenalenyl radicals can form either σ-dimers or π-dimers in the solid state.[xx] All σ-dimers have been found to be diamagnetic as the two radical sites interact strongly and their spins pair up to create an σ-bond. In contrast, in π-dimers, spiro-bis-phenalenyls can couple either diamagnetically (at lower temperatures) or paramagnetically (at higher temperatures).[143a,b] This arises from the fact that the interplanar distance between two π-stacked phenalenyl radicals increases as the temperature is increased. Hence, the overlap of the two singly occupied molecular orbitals (SOMOs) on neighboring phenalenyl units is decreased, which makes spin pairing less favored. In addition, excess of spin density remains on the outer phenalenyl ligands at higher temperatures, which prevents further spin pairing and, consequently, stabilizes the paramagnetic state.

Piers *et al.* have recently synthesized two persistent spirocyclic radicals, **19a** and **19b**, in which a substituted 2,2´-bipyridyl is coordinated to 9-bora-9,10-dihydroanthracene.[147] The radicals **19** can be obtained by treating THF solutions of the respective cationic salts with one equivalent of potassium graphite. The addition of the reducing agent quickly gives rise to dark green/brown solutions

[xx] Some solid state structures of spiro-bis-phenalenyls are heavily distorted and do not readily fall into either of these two categories.

and the extraction of reaction mixture with toluene affords **19a** and **19b** as dark solids.

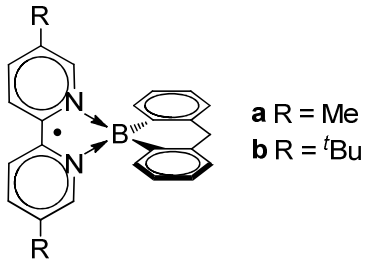

19

Since there are no crystal structure data for radicals **19**, their characterization is based on electron paramagnetic resonance (EPR) spectroscopy and computational studies.[147] Experimentally measured isotropic g-values for **19a** and **19b** were found to be close to 2.0, which is typical for organic π-based radicals containing only light p-block heteroatoms. Furthermore, the simulation of their EPR spectra by using calculated hyperfine coupling constants as initial estimates of the true couplings yielded an excellent match. This confirmed that most of the spin density remains on boron and on the atoms of the substituted 2,2´-bipyridyl ligand. Hence, in these radicals, the spin density is not delocalized over the entire molecular framework. A closer look at the frontier orbitals calculated for **19a** revealed that the SOMO is strongly localized on the 2,2'-bipyridyl ligand and, consequently, there are no conjugative orbital interactions between the two ligands in the molecule.

In addition to the above examples, there are two other well-characterized classes of compounds in the family of stable neutral spirocyclic radicals involving group 13 elements: spiro-bis-boraamidinate radicals (**20**)[145] and spiro-bis-diazabutadiene radicals (**21**). [148] Chivers *et al*. have generated spiro-bis-boraamidinates from their lithium salts by oxidizing them with iodine,[145] wheras spiro-bis-diazabutadiene radicals can be synthesized by reacting an anionic gallium *N*-heterocyclic carbene analogue of diazabutadiene with "GaI",[148a] for example. Other synthetic routes also exist for spiro-bis-diazabutadienes.[148]

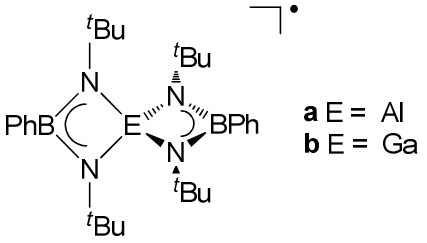

20

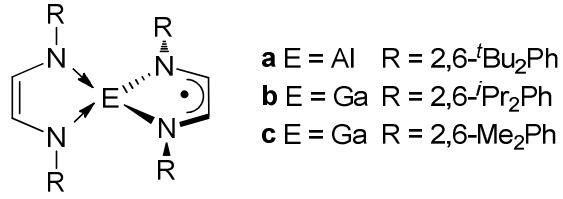

21

X-ray crystal structures of both spiro-bis-boraamidinates[145] and spiro-bis-diazabutadiene radicals have been reported,[148] and they reveal that both compounds adopt spirocyclic geometries in the solid state. However, the two diazabutadiene ligands in **21** exhibit distinctly different metrical parameters,[148a,c]

whereas the structures of spiro-bis-boraamidinate radicals **20** are fully symmetric. Subsequent EPR and computational studies confirmed that the electronic structures of these radicals are totally different. In spiro-bis-boraamidinate radicals, the spin density is distributed uniformly over both ligands,[145] whereas in spiro-bis-diazabutadienes the unpaired electron is essentially localized on only one ligand.[148] The differences in the electronic structures of **20** and **21** naturally originate from the morphologies of their SOMOs. Boraamidinate ligands have an antisymmetric π-type HOMO, which means that the conditions for spiroconjugation are fulfilled (Figure 11, left).[145] In contrast, diazabutadiene ligands have a symmetric HOMO, which means that the SOMO of spiro-bis-diazabutadienes would be doubly degenerate (Figure 11, right). Consequently, spiro-bis-diazabutadiene radicals undergo Jahn-Teller distortion and subsequent localization of the spin.[145] The structures of **20** and **21** are excellent examples of how seemingly small changes in the ligand framework can have a drastic effect on the orbital structure and the distribution of spin density.

4.3 Results and discussion

Although most of the stable neutral spiroconjugated radicals are based on the phenalenyl framework,[143] spiroconjugation is by no means an unique property of these systems as shown in the previous sections of this chapter. In principle, any two chelating ligands that both have antisymmetric π-type frontier orbitals can be used to realize spiroconjugation. However, in order for the ligand to be a useful building block for neutral spiroconjugated radicals, it should also exhibit redox non-innocent behavior and be able to effectively delocalize the unpaired electron over the entire molecular framework.

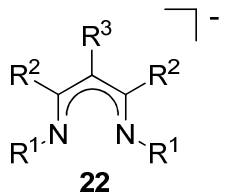

22

The monoanionic *N*,*N'*-chelating *β*-diketiminate (NacNac) ligand (**22**; $R^{1,2,3}$ = H, alkyl, aryl) is known to form a plethora of coordination complexes with a range of different metals.[149] However, there are only a very few reports which describe the redox properties of this ligand framework.[150] This is somewhat surprising as the ligand has a low-energy antisymmetric π-type LUMO that could potentially accept electron density and take part in spiroconjugative interactions. From this background, detailed computational and experimental investigations of the suitability of the NacNac ligand in the synthesis of new spirocyclic main group radicals were initiated. This represents an attractive objective as the versatility and tunability of this particular ligand framework is

ideal for the generation of a new family of paramagnetic coordination compounds. The original results of this work were reported in full in research Paper **IV**.

4.3.1 Computational analysis of the *β*-diketiminate ligand as a new building block for stable main group radicals

In combination with a group 13 element in an oxidation state +III, two NacNac ligands are expected to give rise to spirocyclic cations which can then be reduced to neutral radicals **23-26**. However, cationic 2:1 complexes of the NacNac ligand with group 13 elements are virtually non-existent, the sole characterized member being [**24d**]$^+$, and their redox chemistry is completely uncharted.[151] Consequently, due to the scarcity of the experimental data, computational analyses were done for a number of potential candidates (**a**-**k**), which offered a way to select the most promising systems for further synthetic work.

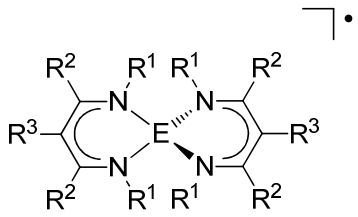

23-26

23 E = B
24 E = Al
25 E = Ga
26 E = In

a R^1 = Me, R^2 = R^3 = H
b R^1 = tBu, R^2 = R^3 = H
c R^1 = Ph, R^2 = R^3 = H
d R^1 = R^2 = Me, R^3 = H
e R^1 = Me, R^2 = tBu, R^3 = H
f R^1 = Me, R^2 = Ph, R^3 = H
g R^1 = tBu, R^2 = Me, R^3 = H
h R^1 = Ph, R^2 = Me, R^3 = H
i R^1 = R^2 =-CHCHCH-, R^3 = H
j R^1 = R^2 =-CHCHCHCH-, R^3 = H
k R^1 = R^2 =-CHCHCHCH-, R^3 = Me

The computational analyses were started by optimizing the geometries of **23-26** at the DFT level. Frequency calculations were performed for all optimized geometries to confirm the nature of stationary points found. These revealed that the majority of the investigated systems are stable minima on the potential energy hypersurface, thereby confirming their viability as synthetic targets. However, it was found that the optimized structures of gallium and indium radicals had lower point groups than their boron and aluminum analogues, indicative of either incomplete or missing spiroconjugation. Consequently, more detailed computational analyses were conducted only for derivatives **23** and **24**.

The investigation of the frontier MOs of **23** and **24** revealed that their SOMOs exhibit spiroconjugation (Figure 12). Furthermore, the SOMOs were found to have two nodal planes which bisect and create a node at the middle carbon atom within both NacNac ligands. This indicates that the -CR^3 substituents will have only an indirect (steric) effect to the properties of spiro-bis-*β*-diketiminates. In contrast, both -NR^1 and -CR^2 atoms make a large contribution to the SOMO, which means that the electronic properties of the target radicals can be readily fine-tuned by varying the substituents at these positions. Substituents that delocalize the spin density the most should be favored as this is expected to increase

the stability of the radicals. In this respect, NacNac ligands with either aryl groups (**c**, **f** and **h**) or neighboring fused rings (**i**–**k**) at R^1 and R^2 positions appeared the most promising candidates. However, it was found that having too bulky substituents at these positions prevents conjugative interactions by introducing structural deformations. Therefore, the aluminum derivative **24j** was chosen as the first synthetic target.

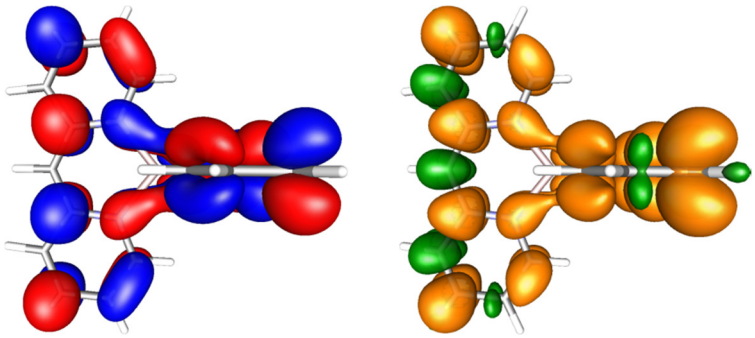

Figure 12. The SOMO (left) and spin density (right) of **24j**. Color code: orange = α spin density, green = β spin density.

4.3.2 Experimental synthesis and characterization of a paramagnetic aluminum spiro-bis-*β*-diketiminate

Treatment of the ligand **27**[152] with 1 equivalent of *n*-BuLi and 0.5 equivalent of $MeAlCl_2$ gave the 2:1 complex **28** as an orange powder in 57% yield (Scheme 1). The methyl group in **28** was easily eliminated by reacting **28** with a stoichiometric amount of either tris(pentafluorophenyl)- or triphenylborane to afford the salts **29a** and **29b** as orange powders in good yields. The desired radical **24j** was obtained by treating the salts **29a** and **29b** with a stoichiometric amount of decamethylcobaltocene or cobaltocene. During mixing, the initially orange red solutions of **29** turned intensely dark and evaporation of the solvent yielded grayish brown solid residues which were analyzed by spectroscopy and computational chemistry.

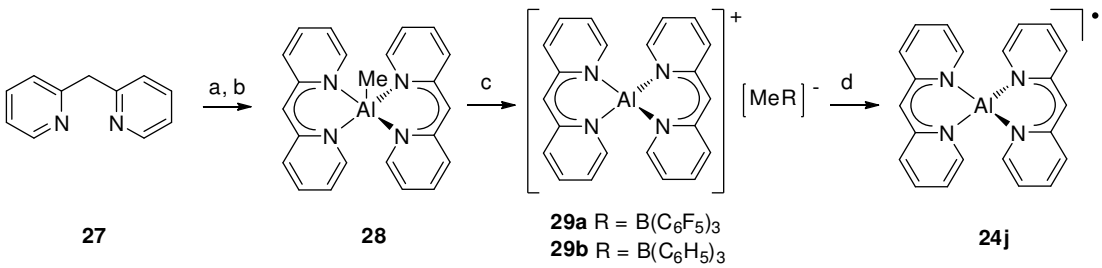

Scheme 1. The synthesis of **24j**. a) 1 eq. *n*-BuLi, THF, -78°C, 1h; b) 0.5 eq. $MeAlCl_2$, THF, -40°C, 1h, 45°C, 45 min, 57%; c) 1 eq. $B(C_6H_5)_3$, CH_2Cl_2, RT, 2 h, 82 % / 1 eq. $B(C_6F_5)_3$, CH_2Cl_2, RT, 2 h, 60%; d) 1 eq. $CoCp^*_2$, CH_2Cl_2, RT, 24 h / 1 eq. $CoCp_2$, CH_2Cl_2, RT, 24 h / 1 eq. K, toluene, RT, 15 min.

All attempts to crystallize **24j** yielded either stacked parallel layers of plate-like red crystals, which were presumably **24j** but unsuitable for X-ray analysis, or the expected reduction by-product (cobaltocenium salt of triphenylmethylborate) as yellow crystals. However, EPR studies supported the identity of **24j** and its stability. The X-band EPR spectrum of **24j** was recorded both in toluene and in the solid state, and it shows a broad singlet with a g-value close to 2.0. Furthermore, the observed EPR signal remained essentially unchanged even after months of storage of the solid residue in an inert atmosphere. Due to the featureless nature of the measured spectrum, the frontier orbital structure and spin density of **24j** were also modeled computationally (Figure 12). The calculations clearly show the presence of spiroconjugation and delocalization of spin density over the entire molecular framework, confirming that **24j** is a ligand-centered radical as desired.

5 CONCLUSIONS

This dissertation combined three different topics in main group chemistry which concentrate on inter- and intramolecular interactions, multiconfigurational character and stable spirocyclic radicals. The focus of the first two chapters was on different bonding interactions between and within molecules, and extensive quantum chemical calculations showed that, for the specific systems in question, the bonding nature cannot solely be assigned in terms of experimental bond length. The aim of the third chapter was to characterize, both experimentally and theoretically, new spirocyclic radicals based on the β-diketiminate ligand.

Closed shell interactions originate from dynamic electron correlation effects, whose modeling requires the use of sophisticated quantum chemical methods. In this respect, the pnictogen-based dimers $X_3Pn\cdots PnX_3$ (Pn = N-Bi; X = F-I) and dithallenes RTlTlR (R = H, Me, ^{t}Bu, Ph) were found to be classical examples of dispersion-bound systems. In the former case, the examined Pn···Pn interactions were found to be sufficiently strong to be used in crystal engineering, whereas in the latter case it was shown that the bonding in the experimentally characterized dithallene can be largely assigned to kinetic stabilization provided by its bulky substituents. In contrast to these findings, the intramolecular weak Ch···Ch interaction in chalcogen dications Ch_8^{2+} (Ch = S, Se) was not found to be dispersion-bound, but the observed bonding results from the interplay of covalent character and complex, repulsive, dynamic electron correlation effects.

The analysis of bonding interactions becomes even more complex when the wave function contains (near) degeneracy effects such as singlet diradical character. In this case, not only dynamic but also static correlation effects need to be treated appropriately using high-level multiconfigurational methods. Of all the systems studied in this dissertation, group 13 dimetallenes REER (E = Al-In; R = H, Me, ^{t}Bu, Ph) and tetrachalcogen tetranitrides Ch_4N_4 (Ch = S, Se) fall in this category. Their multiconfigurational character was found to be closely associated with the key E-E and Ch···Ch interactions that contain an important singlet diradical component that had not been previously recognized. In addi-

tion, the results clearly proved that the E-E and Ch···Ch interactions in these systems are much weaker than conventional double and single bonds, respectively.

Stable neutral radicals can be used as building blocks for novel molecule-based materials with interesting conducting and magnetic properties. However, the number of stable radical families is currently limited and, for this reason, the synthesis of new stable neutral radicals is an important research area. Therefore, the last third of this dissertation was devoted to experimental and computational studies of spirocyclic bis-β-diketiminate radicals. The successful synthesis of the first paramagnetic aluminum β-diketiminate complex gave strong evidence that the β-diketiminate ligand framework can support a singly reduced paramagnetic state and be used to generate a new family of main group radicals. These findings were fully supported by computational analyses.

REFERENCES

1. Lewis, G. N. *J. Am. Chem. Soc*. **1916**, *38*, 762.
2. Stone, A. J. *The Theory of Intermolecular Forces*, Oxford University Press: Oxford, UK, 1997.
3. For some examples, see: (a) Bishop, K. J. M.; Wilmer, C. E.; Soh, S. and Grzybowski, B. A. *Small* **2009**, *5*, 1600. (b) Steed, J. W. and Atwood, J. L. *Supramolecular Chemistry*, John Wiley & Sons: Chicester, UK, 2009.
4. Housecroft, C. E. and Constable, E. C. *Chemistry*, *2nd edition*, Pearson Education: Harlow, UK, 2002, pp 115-116.
5. (a) Allen, T. L.; Fink, W. H. and Power, P. P. *J. Chem. Soc., Dalton Trans*. **2000**, 407. (b) Xie, Y.; Grev, R. S.; Gu, J.; Schaefer, H. F. III; Schleyer, P. v. R.; Su, J.; Li, X.-W. and Robinson, G. H. *J. Am. Chem. Soc*. **1998**, *120*, 3773. (c) Cotton, F. A.; Cowley, A. H. and Feng, X. *J. Am. Chem. Soc*. **1998**, *120*, 1795. (d) Klinkhammer, K. W. *Angew. Chem., Int. Ed. Engl*. **1997**, *36*, 2320.
6. (a) Treboux, G. and Bathelat, J.-C. *J. Am. Chem. Soc*. **1993**, *115*, 4870. (b) Schwerdtfeger, P. *Inorg. Chem*. **1991**, *30*. 1660.
7. (a) Ponec, R.; Yuzhakov, G.; Gironés, X. and Frenking, G. *Organometallics* **2004**, *23*, 1790. (b) Chesnut, B. D. *Heteroat. Chem*. **2003**, *14*, 175. (c) Schnöckel, H. and Himmel, H.-J. *Chem.-Eur. J*. **2003**, *9*, 748. (d) Himmel, H.-J. and Schnöckel, H. *Chem.-Eur. J.* **2002**, *8*, 2397. (e) Bridgeman, A. J. and Ireland, L. R. *Polyhedron* **2001**, *20*, 2851. (f) Takagi, N.; Schmidt, M. W. and Nagase, S. *Organometallics* **2001**, *20*, 1646. (g) Molina, J. M.; Dobado, J. A.; Heard, G. I.; Bader, R. F. W. and Sundberg, M. R. *Theor. Chem. Acc.* **2001**, *105*, 365. (h) Grützmacher, H. and Fässler, T. F. *Chem.-Eur. J.* **2000**, *6*, 2317.
8. (a) Trinquier, G. and Malrieu, J.-P. *J. Am. Chem. Soc*. **1987**, *109*, 5303. (b) Malrieu, J.-P. and Trinquier, G. *J. Am. Chem. Soc*. **1989**, *111*, 5916. (c) Carter, E. A. and Goddard, W. A. III *J. Phys. Chem*. **1986**, *90*, 998.
9. Zhu, Z.; Fischer, R. C.; Ellis, B. D.; Rivard, E.; Merrill, W. A.; Olmstead, M. M.; Power, P. P.; Guo, J. D.; Nagase, S. and Pu, L. *Chem.-Eur. J*. **2009**, *15*, 5263.
10. For some recent reviews, see: (a) Glaser, T. *Chem. Commun*. **2011**, 116. (b) Yakhmi, K. *J. Bull. Mater. Sci*. **2009**, *32*, 217. (c) Fourmiqué, M. *Struct. Bond*. **2008**, *126*, 181. (d) Fourmiqué, M. and Batail, P. *Chem. Rev*. **2004**, *104*, 5379.
11. (a) Nascimento, M. A. C. *Theoretical Aspects of Heterogeneous Catalysis*, Kluwer Academic Publishers: Dordrecht, Netherlands, 2001, pp 77-108. (b) Tuma, C. and Sauer, J. *Phys. Chem. Chem. Phys.* **2006**, *8*, 3955.
12. Grimme, S.; Diedrich, C. and Korth, M. *Angew. Chem., Int. Ed*. **2006**, *45*, 625.

13. McNaught, A. D. and Wilkinson, A. *IUPAC Compendium of Chemical Terminology, 2nd editon (the "Gold Book")*, Blackwell Scientific Publications: Oxford, UK, 1997. XML on-line corrected version: http://goldbook.iupac.org (2006-); Created by Nic, M.; Jirat, J. and Kosata, B. updates compiled by Jenkins, A.

14. (a) Grimme, S. *Angew. Chem., Int. Ed.* **2008**, *47*, 3430. (b) Hunter, C. A. and Sanders, J. K. M. *J. Am. Chem. Soc.* **1990**, *112*, 5525.

15. (a) Kodama, Y.; Nishinata, K.; Nishio, M. and Nagakawa, N. *Tetrahedron Lett.* **1977**, 2105. (b) Nishio, M.; Hirota, M. and Umezawa, Y. *The CH/π Interaction*, Wiley-VCH: New York, USA, 1998.

16. For some examples, see: (a) Lari, A.; Gleiter, R. and Rominger, F. *Eur. J. Org. Chem.* **2009**, *14*, 2267. (b) Lari, A.; Bleiholder, C.; Rominger, F. and Gleiter, R. *Eur. J. Org. Chem.* **2009**, *17*, 2765. (c) Bleiholder, C.; Gleiter, R.; Werz D. B. and Köppel, H. *Inorg. Chem.* **2007**, *46*, 2249. (d) Bleiholder, C.; Werz, D. B.; Köppel, H. and Gleiter, R. *J. Am. Chem. Soc.* **2006**, *128*, 2666. (e) Werz, D. B.; Staeb, T. H.; Benisch, C.; Rausch, B. J.; Rominger, F. and Gleiter, R. *Org. Lett.* **2002**, *4*, 339. (f) Werz, D. B.; Gleiter, R. and Rominger, F. *J. Am. Chem. Soc.* **2002**, *124*, 10638.

17. For some examples, see: (a) Kurzbach, D.; Sharma, A.; Sebastiani, D.; Klinkhammer, K. W. and Hinderberger, D. *Chem. Sci.* **2011**, *2*, 473. (b) Schoeller, W. W. *J. Mol. Struct. Theochem* **2010**, *957*, 66. (c) Heard, P. J. *Main Group Dithiocarbamate Complexes*, in Progress in Inorganic Chemistry, Karlin K. D. (Ed.), John Wiley & Sons, Inc: Hoboken, USA, 2005, pp 28. (d) Klinkhammer, K. W. and Pyykkö, P. *Inorg. Chem.* **1995**, *34*, 4134. (e) Scheiner, S. *Acc. Chem. Res*. DOI: 10.1021/ar3001316.

18. (a) Pyykkö, P. *Angew. Chem., Int. Ed.* **2004**, *43*, 4412. (b) Pyykkö P. *Chem. Rev.* **1997**, *97*, 597. (c) Schmidbaur, H. *Gold Bull.* **2000**, *33*, 3. (d) Schmidbaur, H. and Schier, A. *Chem. Soc. Rev.* **2008**, *37*, 1931.

19. (a) Kim, M.; Taylor, T. J. and Gabbai, F. P. *J. Am. Chem. Soc.* **2008**, *130*, 6333. (b) Joszai, R.; Beszeda, I.; Benyei, A. C.; Fischer, A.; Kovacs, M.; Maliarik, M.; Nagy, P.; Shchukarev, A. and Toth, I. *Inorg. Chem.* **2005**, *44*, 9643. (c) Hermann, H. L.; Boche, G. and Schwerdtfeger, P. *Chem.-Eur. J.* **2001**, *7*, 5333. (d) Pyykkö, P. and Straka, M. *Phys. Chem. Chem. Phys*. **2000**, *2*, 2489.

20. Bardají, M. and Laguna, A. *Eur. J. Inorg. Chem*. **2003**, *17*, 3069.

21. For a review, see: Katz, M. J.; Sakai, K. and Leznoff, D. B. *Chem. Soc. Rev.* **2008**, *37*, 1884.

22. Cangelosi, V. M.; Pitt, M. A.; Vickaryous, W. J.; Allen C. A.; Zakharov, L. N. and Johnson D. W. *Cryst. Growth & Des.* **2010**, *10*, 3531.

23. Helgaker, T.; Jørgensen P. and Olsen, J. *Molecular Electronic-Structure Theory*, John Wiley & Sons: Chicester, UK, 2004.

24. Møller, C. and Plesset, M. S. *Phys. Rev.* **1934**, *46*, 618.

25. Sherrill, C. D. and Schaefer, H. F. III *Adv. Quantum Chem*. **1999**, *34*, 143.

26. (a) Deegan, M. J. O. and Knowles, P. J. *Chem. Phys. Lett.* **1994**, *227*, 321. (b) Hampel, C.; Peterson, K. and Werner, H.-J. *Chem. Phys. Lett.* **1992**, *190*, 1. (c) Raghavachari, K.; Trucks, G. W.; Pople, J. A. and Head-Gordon, M. *Chem. Phys. Lett.* **1989**, *157*, 479.

27. (a) Janowski, T. and Pulay, P. *Chem. Phys. Lett.* **2007**, *447*, 27. (b) Tsuzuki, S.; Uchimaru, T.; Matsumura, K.; Mikami, M. and Tanabe, K. *Chem. Phys. Lett.* **2000**, *319*, 547. (c) Jaffe, R. L. and Smith, G. D. *J. Chem. Phys.* **1996**, *105*, 2780. (d) Hobza, P.; Selzle, H. L. and Schlag, E. W. *J. Phys. Chem.* **1996**, *100*, 18790.

28. (a) Reinhold F. F. *J. Chem. Phys.* **2010**, *133*, 174113. (b) Szabados, Á. *J. Chem. Phys*. **2006**, *125*, 214105. (c) Grimme, S. *J. Chem. Phys*. **2003**, *118*, 9095.

29. (a) Tao, F. *Int. Rev. Phys. Chem*. **2001**, *20*, 617. (b) van Duijneveldt, F. B.; van Duijneveldt-van de Rijdt, J. G. C. M. and van LentheJoop, H. *Chem. Rev*. **1994**, *94*, 1873.

30. Boys, S. F. and Bernardi, F. *Mol. Phys*. **1970**, *19*, 553.

31. Werner, H. and Pflüger, K. *On the Selection of Domains and Orbital Pairs in Local Correlation Treatments*, in Annual Reports in Computational Chemistry, Spellmeyer, D. C. (Ed.), Elsevier: New York, USA, 2006, pp 53-80.

32. Pople J. A. and Head-Gordon M. *J. Chem. Phys.* **1987**, *87*, 5968.

33. Bartlett, R. J. and Musial M. *Rev. Mod. Phys*. **2007**, *79*, 291.

34. Koch, W. and Holthausen, M. C. A. *Chemist's Guide to Density Functional Theory, 2nd edition*, Wiley VCH: Weinheim, German, 2001.

35. Hohenberg, P. and Kohn, W. *Phys. Rev*. **1964**, *136*, B864.

36. Kohn, W. and Sham, L. *Phys. Rev*. **1965**, *140*, A1133.

37. Johnson, E. R. and DiLabio, G. A. *Chem. Phys. Lett*. **2006**, *419*, 333.

38. Williams, H. L. and Chabalowski, C. F. *J. Phys. Chem. A* **2001**, *105*, 646.

39. (a) Grimme, S. *J. Comput. Chem*. **2004**, *25*, 1463. (b) Grimme, S. *J. Comput. Chem*. **2006**, *27*, 1787. (c) Grimme, S.; Antony, J.; Ehrlich, S. and Krieg, H. *J. Chem. Phys*. **2010**, *132*, 154104.

40. (a) Becke, A. D. and Johnson, E. R. *J. Chem. Phys*. **2005**, *122*, 154104. (b) Becke, A. D. and Johnson, E. R. *J. Chem. Phys*. **2005**, *123*, 154101.

41. Tkatchenko, A. and Scheffler, M. *Phys. Rev. Lett*. **2009**, *102*, 073005.

42. Sato, T. and Nakai, H. *J. Chem. Phys*. **2009**, *131*, 224104.

43. (a) Goll, E.; Leininger, T.; Manby, F. R.; Mitrushchenkov, A.; Werner, H.-J. and Stoll, H. *Phys. Chem. Chem. Phys*. **2008**, *10*, 3353. (b) Gerber, I. C. and Ángyán, J. G. *J. Chem. Phys.* **2007**, *126*, 044103. (c) Goll, E.; Werner, H.-J. and Stoll, H. *Phys. Chem. Chem. Phys.* **2005**, *7*, 3917. (d) Ángyán, J. G.; Gerber, I. C.; Savin, A. and Toulouse, J. *Phys. Rev. A* **2005**, *72*, 012510.

44. (a) Dion, M.; Rydberg, H.; Schröder, E.; Langreth, D. C. and Lundqvist, B. I. *Phys. Rev. Lett*. **2004**, *92*, 246401. (b) Andersson, Y.; Langreth, D. C. and Lundqvist, B. I. *Phys. Rev. Lett*. **1996**, *76*, 102.

45. (a) Zhao, Y. and Truhlar, D. G. *J. Phys. Chem. C* **2008**, *112*, 4061. (b) Zhao, Y. and Truhlar, D. G. *Theor. Chem. Acc.* **2008**, *120*, 215. (c) Zhao, Y.; Schultz, N. E. and Truhlar, D. G. *J. Chem. Theory Comput*. **2006**, *2*, 364. (d) Xu, X. and Goddard, W. *A Proc. Natl. Acad. Sci. U. S. A*. **2004**, *101*, 2673.

46. For a review, see: Grimme, S.; Goerick, L. and Fink, R. F. *Spin-Component-Scaled Electron Correlation Methods*, in *Comput. Mol. Sci*. **2012**, doi: 10.1002/wcms.1110.

47. (a) Distasio, R. A. Jr. and Head-Gordon, M. *Mol. Phys*. **2007**, *105*, 1073. (b) Hill, G. J. and Platts, J. A. *J. Chem. Theory Comput*. **2007**, *3*, 80.

48. (a) Pitoňák, M.; Řezáč, J. and Hobza, P. *Phys. Chem. Chem. Phys*. **2010**, *12*, 9611. (b) Takatani, T.; Hohenstein, E. G. and Sherrill, C. D. *J. Chem. Phys*. **2008**, *128*, 124111.

49. Hellweg, A.; Grün, S. A. and Hättig C. *Phys. Chem. Chem. Phys*. **2008**, *10*, 4119.

50. Grimme, S. and Ugorodina, E. I. *Chem. Phys*. **2004**, *305*, 223.

51. Christiansen, O.; Koch, H. and Jørgensen, P. *Chem. Phys. Lett*. **1995**, *243*, 409.

52. Jung, Y.; Lochan, R. C.; Dutoi, A. D. and Head-Gordon M. *J. Chem. Phys*., **2004**, *121*, 9793.

53. Monari, A.; Bendazzoli, G. L.; Evangelisti, S.; Angeli, C.; BenAmor, N.; Borini, S.; Maynau, D. and Rossi, E. *J. Chem. Theory Comput.* **2007**, *3*, 477.

54. Dunning, T. H. Jr. *J. Phys. Chem. A* **2000**, *104*, 9062.

55. For some examples, see: (a) Kruse, H. and Grimme, S. *J. Chem. Phys.* **2012**, *136*, 154101. (b) Jensen F. *J. Chem. Theory Comput*. **2010**, *6*, 100. (c) Valdés, H.; Klusák, V.; Pitoňák, M.; Exner, O.; Starý, O.; Hobza, P. and Rulíšek, L. *J. Comput. Chem*. **2008**, *29*, 861.

56. Halkier, A.; Klopper, W.; Helgaker, T.; Jørgensen, P. and Taylor, P. R. *J. Chem. Phys*. **1999**, *111*, 9157.

57. Sherrill, C. D.; Takatani, T. and Hohenstein, E. G. *J. Phys. Chem. A* **2009**, *113*, 10146.

58. Werner H.-J. and Schütz, M. *J. Chem. Phys*. **2011**, *135*, 144116.

59. Boys. S. F. *in Quantum Theory of Atoms, Molecules, and the Solid State*, Löwdin, P. O. (Ed.), Academic Press: New York, USA, 1966, p. 253.

60. Pipek, J. and Mezey, P. G. *J. Chem. Phys*. **1989**, *90*, 4916.

61. (a) Reed, A. E. and Weinhold F. *J. Chem. Phys*. **1985**, *83*, 1736. (b) Werner H.-J. and Mata R. A. *Mol. Phys.* **2007**, *105*, 2753.

62. James, W. and Boughton, P. P. *J. Comput. Chem.* **1993**, *14*, 736.

63. Runeberg, N.; Schütz, M. and Werner, H.-J. *J. Chem. Phys*. **1999**, *110*, 7210.

64. For a review, see: Jeziorski, B.; Moszynski, R. and Szalewicz, K. *Chem. Rev*. **1994**, 94, 1887.

65. (a) Kendall, R. A.; Chalasiński, G.; Kłos J.; Bukowski, R.; Severson, M. W.; Szczęśniak, M. and Cybulski, S. M. *J. Chem. Phys*. **1998**, *108*, 3235. (b) Cybulski, S. M.; Burcl, R.; Szczęśniak, M. M. and Chałasiński, G. *J. Chem. Phys*. **1996**, *104*, 7997. (c) Moszyński, R.; Cybulski, S. M. and Chałasiński, G. *J. Chem. Phys*. **1994**, *100*, 4998. (d) Cybulski, S. M.; Chałasiński, G. and Moszyński R. *J. Chem. Phys*. **1990**, *92*, 4357.

66. Langlet, J.; Caillet, J.; Bergés, J. and Reinhardt, P. *J. Chem Phys* **2003**, *118*, 6157.

67. Ganesamoorthy, C.; Balakrishna, M. S.; Mague, J. T. and Tuononen, H. M. *Inorg. Chem.* **2008**, *47*, 7035.

68. Batail, P.; Grandjean, D.; Dudragne, F. and Michaud, C. *Acta Cryst*. **1975**, *B31*, 1367.

69. Kuhn, N.; Fawzi, R.; Steimann, M. and Wiethoff, J. *Chem. Ber*. **1996**, *129*, 479.

70. Avtomonov, E. V.; Megges, K.; Wocadlo, S. and Lorberth, J. *J. Organomet. Chem*. **1996**, *524*, 253.

71. (a) Yeh, W.; Seino, H.; Amitsuka, T.; Ohba, S.; Hidai, M. and Mizobe, Y. *J. Organomet. Chem*. **2004**, *689*, 2338. (b) Jones, C.; Junk, P. C.; Richards, A. F. and Waugh, M. *New. J. Chem.* **2002**, *26*, 1209.

72. Becker, I.; Windhaus, M. and Mattes, R. *Z. Naturforsch. B: Chem. Sci*. **1994**, *49*, 870.

73. Baker, W. A. and Williams, D. E. *Acta Cryst*. **1978**, *B34*, 3739.

74. (a) Kozulin, A. T.; Gogolev, A. V. and Shishkin, S. G. *Izv. Vyssh. Uchebdn. Zaved.* **1977**, *20*, 42. (b) Kozulin, A. T.; Gogolev, A. V.; Karmanov, V. I. and Murtsovkin, V. A. *Opt. Spektrosk.* **1973**, *34*, 1218.

75. (a) Cameron, T. S.; Deeth, R. J.; Dionne, I.; Du, H.; Jenkins, H. D. B.; Krossing, I.; Passmore, J. and Roobottom, H. K. *Inorg. Chem*. **2000**, *39*, 5614. (b) Ciolowski, J. and Gao, X. *Int. J. Quant. Chem*. **1997**, *65*, 609.

76. (a) Tang, T. H.; Bader, R. F. W. and MacDougall, P. J. *Inorg. Chem*. **1985**, *24*, 2047. (b) Gillespie, R. J. *J. Chem. Soc. Rev*. **1979**, *8*, 315.

77. (a) Pritchina, E. A.; Gritsan N. P.; Zibarev, A. V. and Bally, T. *Inorg. Chem*. **2009**, 48, 4075. (b) Chung G. and Lee, D. *J. Mol. Struct. Theochem* **2002**, *582*, 85. (c) Bridgeman A. J.; Cavigliasso G.; Ireland, L. R. and Rothery, J. *J. Chem. Soc., Dalton Trans*., **2001**, 2095. (d) Scherer, W.; Spegler, M.; Pederson, B.; Tafipolsky, M.; Hieringer, W.; Reinhard, B.; Downs, A. J. and McGrady G. S. *Chem. Commun*. **2000**, 635. (e) Suontamo R. J. and Laitinen, R. S. *J. Mol. Struct. Theochem* **1995**, 336, 55. (f) Brown, A. S. and Smith V. H. Jr. *J. Chem. Phys*. **1993**, 99, 1837. (g) Findlay, R. H.; Palmer, M. H.; Downs A. J.; Egdell, R. G. and Evans, R. *Inorg. Chem*. **1980**, *19*, 1307. (h) Tanaka, K.; Yamabe, T.; Tachibana, A.; Kato, H. and Fukui, K. *J. Phys. Chem*., **1978**, *82*, 2121. (i) Salahub, D. R. and Messmer, R. P. *J. Chem. Phys*. **1976**, *64*, 2039. (j) Gopinathan, M. S. and Whitehead, M. A. *Can. J. Chem*. **1975**, *53*, 1343. (k) Gleiter, R. *J. Chem. Soc. A* **1970**, 3174. (l) Lu, C.-S. and Donohue, J. *J. Am. Chem. Soc*. **1944**, *66*, 818.

78. Chivers, T; Hilts, R. W.; Jin, P.; Chen, Z. and Lu, X. *Inorg. Chem*. **2010**, *49*, 3810.

79. (a) Maaninen, A.; Laitinen, R. S.; Chivers, T. and Pakkanen, T. A. *Inorg. Chem*. **1999**, *38*, 3450. (b) Folkerts, H.; Neumüller, B. and Dehnicke, K. *Z. Anorg. Allg. Chem*. **1994**, *620*, 1011. (c) DeLucia, M. L. and Coppens, P. *Inorg. Chem*. **1978**, *17*, 2336. (d) Bärnighausen, von H. and Volkmann, von T. *Acta Cryst*. **1966**, *21*, 571. (e) Sharma, B. D. and Donohue, J. *Acta Cryst*. **1963**, *16*, 891. (f) Jander, J. and Doetsch, V. *Angew. Chem*. **1958**, *70*, 704. (g) Clark, D. *J. Chem. Soc*. **1952**, 1615. (h) Gregory, M. *J. Pharm*. **1835**, *21*, 315.

80. (a) Chivers, T.; Edwards, M. and Parvez, M. *Inorg. Chem*. **1992**, *31*, 1861. (b) Burford, N.; Chivers, T. and Richardson, J. F. *Inorg. Chem*. **1983**, *22*, 1482. (c) Burford, N.; Chivers, T.; Codding, P. W. and Oakley R. T. *Inorg. Chem*. **1982**, *21*, 982. (d) Ernest, I.; Holick, W.; Rihs, G.; Schomburg, D.; Shoham, G.; Wenkert, D. and Woodward, R. B. *J. Am. Chem. Soc*. **1981**, *103*, 1540.

81. (a) Beck, J. and Muller-Buschbaum, K. *Z. Anorg. Allg. Chem*. **1997**, *623*, 409. (b) Collins, M. J.; Gillespie, R. J. and Sawyer J. F. *Acta Cryst*. **1988**, *C44*, 405. (c) McMullan R. K.; Prince, D. J. and Corbett, J. D. *Inorg. Chem*. **1971**, *10*, 1749.

82. Pyykkö, P. and Tamm, T. *Organometallics* **1998**, *17*, 4842.

83. (a) Goldberg, D. E.; Harris, D. H.; Lappert, M. F. and Thomas, K. M. *J. Chem. Soc., Chem. Commun*. **1976**, 261. (b) Davidson, P. J. and Lappert, M. F. *J. Chem. Soc., Chem. Commun*. **1973**, 317.

84. (a) Wang, Y. and Robinson, G. H. *Chem. Commun*. **2009**, 5201. (b) Sasamori, T. and Tokitoh, N. *Dalton Trans*. **2008**, 1395. (c) Rivard, E. and Power, P. P. *Inorg. Chem*. **2007**, *46*, 10047. (d) Weidenbruch, M. *Angew. Chem., Int. Ed*. **2005**, *44*, 514. (e) Weidenbruch, M. *Angew. Chem., Int. Ed*. **2003**, *42*, 2222. (f) Power, P. P. *Chem. Commun*. **2003**, 2091. (g) Power, P. P. *Chem. Rev*. **1999**, *99*, 3463.

85. Wright, R. J.; Phillips, A. D.; Hino, S. and Power, P. P. *J. Am. Chem. Soc*. **2005**, *127*, 4794.

86. Pyykkö, P.; Straka, M. and Tamm, T. *Phys. Chem. Chem. Phys*. **1999**, *1*, 3441.

87. For a review, see: Breher, F. *Coord. Chem. Rev*. **2007**, *215*, 1007.

88. (a) Bally, T. and Borden, W. T. *Encyclopedia of Computational Chemistry*, Schleyer, P. v., (Ed.), Wiley: New York, USA, 1998, pp 708-722. (b) Borden, W. T. *Diradicals*; Borden, W. T., (Ed.), Wiley: New York, USA, 1982. (c) Salem, L. and Rowland, C. *Angew. Chem., Int. Ed. Engl*. **1972**, *11*, 92.

89. (a) Sinova, J. and Žutić, I. *Nature Mater.* **2012**, *11*, 368 (b) Wolf, S. A.; Awschalom, D. D.; Buhrman, R. A.; Daughton, J. M.; Molnár, S. von.; Roukes, M. L.; Chtchelkanova, A. Y. and Treger, D. M. *Science* **2001**, *294*, 1488.

90. Niecke, E.; Fuchs, A.; Baumeister, F.; Nieger, M. and Schoeller, W. W. A. *Angew. Chem., Int. Ed. Engl*. **1995**, *34*, 555.

91. Amii, H.; Vranicar, L.; Gornitzka, H.; Bourissou, D. and Bertrand G. *J. Am. Chem. Soc.* **2004**, *126*, 1344.

92. Rodriguez, A.; Tham, F. S.; Schoeller, W. W. and Bertrand, G. *Angew. Chem., Int. Ed.* **2004**, *43*, 4876.

93. Björn, O. R. *Multiconfigurational (MC) Self-Consistent Field (SCF) Theory*, in European Summer School of Quantum Chemistry 2009, Book II, 6th edition, Widmark, P.-O. (Ed.), Media-Tryck, KC: Lund, Sweden, 2009, pp 241-311.

94. (a) Hrovat, D. A. and Borden, W. T. *J Mol. Struct. Theochem* **1997**, *398*, 211. (b) Bally, T. and Borden, W. T. *Calculations on Open-Shell Molecules: a Beginner's Guide*, in Reviews in Computational Chemistry, Lipkowitz, K. B. and Boyd, D. B. (Ed.), Wiley-VCH: New York, USA, 1999, pp 1-97. (c) Rajca, A. *Chem. Rev*. **1994**, *94*, 871. (d) Dougherty, D. A. *Acc. Chem. Res*. **1991**, *24*, 88.

95. (a) Abe, M.; Adam, W.; Hara, M.; Hattori, M.; Majima, T.; Nojima, M.; Tachibana, K. and Tojo, S. *J. Am. Chem. Soc*. **2002**, *124*, 6540. (b) Abe, M.; Adam, W.; Heidenfelder, T.; Nau, W. M. and Zhang, X. *J. Am. Chem. Soc*.

2000, *122*, 2019. (c) Adam, W.; Borden, W. T.; Burda, C.; Foster, H.; Heidenfelder, T.; Heubes, M.; Hrovat, D. A.; Kita, F.; Lewis, S. B.; Scheutzow, D. and Wirz, J. *J. Am. Chem. Soc*. **1998**, *120*, 593.

96. (a) Reyes, M. B.; Lobkovsky, E. B. and Carpenter, B. K. *J. Am. Chem. Soc*. **2002**, *124*, 641. (b) Staroverov, V. N. and Davidson, E. R. *J. Am. Chem. Soc*. **2000**, *122*, 186.

97. Piotrowiak, P.; Strati, G.; Smirnov, S. N.; Warman, J. M. and Schuddeboom, W. *J. Am. Chem. Soc.* **1996**, *118*, 8981.

98. Paci, I.; Johnson, J. C.; Chen, X.; Rana, G.; Popovic, D.; David, D. E.; Nozik, A. J.; Ratner, M. A. and Michl, J. *J. Am. Chem. Soc*. **2006**, *128*, 16546.

99. Tuononen H. M. *EPR Spectroscopic and Quantum Chemical Studies of Some Inorganic Main Group Radicals, Research Report No. 114*, in Department of Chemistry, University of Jyväskylä - Research Report Series, Jyväskylä, Finland, 2005, p. 56.

100. Kamada, K.; Ohta K.; Shimizu, A.; Kubo T.; Kishi, R.; Takahashi H.; Botek, E.; Champagne, B. and Nakano, M. *J. Phys. Chem. Lett*. **2010**, *1*, 937.

101. (a) Bachler, V.; Olbrich, G.; Neese, F. and Wieghardt, K. *Inorg. Chem*. **2002**, *41*, 4179. (b) Hrovat, D. A.; Duncan, J. A. and Borden W. T. *J. Am. Chem. Soc*. **1999**, *121*, 169.

102. Nakano, M.; Kishi, R.; Nakagawa, N.; Ohta S.; Takahashi, H.; Furukawa, S.-I.; Kamada, K.; Ohta, K.; Champagne, B.; Botek E.; Yamada, S. and Yamaguchi, K. *J. Phys. Chem. A* **2006**, *110*, 4238.

103. Seierstad, M.; Kinsinger, C. R. and Cramer, C. J. *Angew. Chem., Int. Ed*. **2002**, *41*, 3894.

104. Dutoi, A. D.; Jung, Y. and Head-Gordon, M. *J. Phys. Chem. A* **2004**, *108*, 10270.

105. Hayes, E. F. and Siu, A. K. Q. *J. Am. Chem. Soc*. **1971**, *93*, 2090.

106. (a) Dohnert, D. and Koutecky, J. *J. Am. Chem. Soc*. **1980**, *102*, 1789. (b) Flynn, C. R. and Michl, J. *J. Am. Chem. Soc*., **1974**, 96, 3280.

107. Löwdin, P.-O. *Phys. Rev*. **1955**, *97*, 1474.

108. Gordon, M. S.; Schmidt, M. W.; Chaban, G. M.; Glaesemann, K. R.; Steevens, W. J. and Gonzalez, C. *J. Chem. Phys*. **1999**, *110*, 4199.

109. Noodleman, L. *J. Chem. Phys*. **1981**, *74*, 5737.

110. Gräfenstein, J.; Kraka, E.; Filatov, M. and Cremer, D. *Int. J. Mol. Sci*. **2002**, *3*, 360.

111. Roos, B. E.; Taylor, P. R. and Siegbahn, P. E. M. *Chem. Phys*. **1980**, *48*, 157.

112. Olsen, J.; Roos, B. O.; Jørgensen, P. and Jensen, H. J. A. *J. Chem. Phys*. **1988**, *89*, 2185.

113. Andersson, K.; Malmqvist, P.-Å. and Roos, B. O. *J. Chem. Phys*., **1992**, *96*, 1218.

114. (a) Werner, H.-J. and Knowles, P. J. *J. Chem. Phys*. **1988**, *89*, 5803. (b) Knowles, P. J. and Werner, H.-J. *Phys. Lett*. **1988**, *145*, 514.

115. For some examples, see: (a) Kállay, M.; Szalay, P. G. and Surján P. R. *J. Chem. Phys*. **2002**, *117*, 980. (b) Mahapatra, U. S.; Datta, B. and Mukherjee, D. *Mol. Phys*. **1998**, *94*, 157.

116. (a) Werner, H.-J.; Kállay, M. and Gauss, J. *J. Chem. Phys*. **2008**, *128*, 034305. (b) Pople, J.; Seeger, R. and Krishnan, R. *Int. J. Quant. Chem*. **1977**, 12, 149.

117. Krossing, I. *Structure and Bonding of the Neutral Chalcogens and Their Polyatomic Cations*, in Handbook of Chalcogen Chemistry: New Perspectives in Sulfur, Selenium and Tellurium, Devillanova, F. A. (Ed.), RSC Publishing: Cambridge, UK, 2007, pp 381-416.

118. Contreras-García, J.; Johnson, E. R.; Keinan, S.; Chaudret, R.; Piquemal, J.-P.; Beratan, D. N. and Yang, W. *J. Chem. Theory Comput*. **2011**, *7*, 625.

119. Almond, M. J.; Forsyth, G. A.; Rice, D. A.; Downs, A. J.; Jeffery, T. L. and Hagen, K. *Polyhedron* **1989**, *8*, 2631.

120. (a) Grigsly, W. J. and Power, P. P. *Chem. Commun*. **1996**, 2235. (b) Moezzi, A.; Olmstead, M. M. and Power, P. P. *J. Am. Chem. Soc*. **1992**, *14*, 2715. (c) Berndt, A.; Klusik, H. and Fichtner, W. *J. Organomet. Chem*. **1981**, *222*, C25. (d) Klusik, H. and Berndt, A. *Angew. Chem., Int. Ed. Engl*. **1981**, *20*, 870.

121. (a) Pluta, C.; Pörschke, K.-R.; Krüger, C. and Hildenbrand, K. *Angew. Chem., Int. Ed. Engl*. **1993**, *32*, 388. (b) Uhl, W.; Vester, A.; Kaim, W. and Poppe, J. *J. Organomet. Chem*. **1993**, *454*, 9. (c) He, X.; Bartlett, R. A.; Olmstead, M. M.; Ruhlandt-Senge, K.; Sturgeon, B. E. and Power, P. P. *Angew. Chem., Int. Ed. Engl*. **1993**, *32*, 717.

122. Su, J.; Li, X.-W.; Crittendon, R. C. and Robinson, G. H. *J. Am. Chem. Soc*. **1997**, *119*, 5471.

123. Hardman, N. J.; Wright, R. J.; Phillips, A. D. and Power, P. P. *Angew. Chem., Int. Ed*. **2002**, *41*, 2842.

124. Zhu, Z.; Fischer, R. C.; Ellis, B. D.; Rivard, E.; Merrill, W. A.; Olmstead, M. M.; Power, P. P.; Guo, J. D.; Nagase, S. and Pu, L. *Chem.-Eur. J*. **2009**, *15*, 5263.

125. Wright, R. J.; Phillips, A. D.; Hardman, N. J. and Power, P. P. *J. Am. Chem. Soc*. **2002**, *124*, 8538.

126. Wright, R. J.; Phillips, A. D. and Power, P. P. *J. Am. Chem. Soc.* **2003**, *125*, 10784.

127. Knight, L. B., Jr.; Kerr, K.; Miller, P. K. and Arrington, C. A. *J. Phys. Chem.* **1995**, *99*, 16842.

128. For a review, see: Ratera, I. and Veciana, J. *Chem. Soc. Rev*. **2012**, *41*, 303.

129. Veciana, J. and Ratera I. *Polychlorotriphenylmethyl Radicals: Towards Multifunctional Molecular Materials,* in Stable Radicals Fundamental and Applied Aspects of Odd-Electron Compounds, Hicks, R. G. (Ed.), Wiley: Chichester, UK, 2010, pp 33-80.

130. For a review, see: Hicks, R. G. *Org. Biomol. Chem*. **2007**, *5*, 1321.

131. For a review, see: Power, P. P. *Chem. Rev*. **2003**, *103*, 789.

132. For a review, see: Miller, J. S. *Adv. Mater*. **2002**, *14*, 1105.

133. For a review, see: Griller, D. and Ingold, K. U. *Acc. Chem. Res*. **1976**, *9*, 13.

134. Ballester, M.; Riera, J.; Castafier, J.; Badfa, C. and Monsó, J. M. *J. Am. Chem. Soc*. **1971**, *93*, 2215.

135. (a) Ballester, M.; Pascual, I.; Riera, J. and Castaner J. *J. Org. Chem*. **1991**, *56*, 217. (b) Ballester, M.; Castaner J.; Riera, J. and Pascual, I. *J. Am. Chem. Soc*. **1984**, *106*, 3365.

136. For a review, see: Reid, D. H. *Q. Rev., Chem. Soc*. **1965**, 19, 274.

137. Goto, K.; Kubo, T.; Yamamoto, K.; Nakasuji, K.; Sato, K.; Shiomi, D.; Takui, T.; Kubota, M.; Kobayashi, T.; Yakusi, K. and Ouyang, J. *J. Am. Chem. Soc.* **1999**, *121*, 1619.

138. (a) Thépot, J. Y. and Lapinte, C. *J. Organomet. Chem*. **2002**, *656*, 146. (b) Janiak, C.; Weimann, R. and Gorlitz, F. *Organometallics*, **1997**, 16, 4933. (c) Sitzmann, H.; Bock, H.; Boese, R.; Dezember, T.; Havlas, Z.; Kaim, W.; Moscherosch, M. and Zanathy, L. *J. Am. Chem. Soc*. **1993**, *115*, 12003. (d) Kieslich, W. and Kurreck, H. *J. Am. Chem. Soc*. **1984**, *106*, 4328.

139. For some examples, see: (a) Barth, T.; Kanellakopulos, B.; Krieger, C. and Neugebauer, F. A. *J. Chem. Soc., Chem. Commun*. **1993**, 1626. (b) Krieger, C.; Peraus, G. and Neugebauer, F.A. *Acta Cryst., Sect. C: Cryst. Struct. Commun.* **1995**, *51*, 1420. (c) Ballester, M.; Castaner, J. and Olivella, S. *Tetrahedron Lett.* **1974**, 615.

140. Gomberg, M. *J. Am. Chem. Soc*. **1900**, *22*, 757.

141. For a review, see: Rawson, J. M.; Alberola, A. and Whalley, A. *J. Mater. Chem*. **2006**, *16*, 2560.

142. Schweig, A.; Weidnel, U.; Hellwinkel, D. and Krapp, W. *Angew. Chem., Int. Ed. Engl*. **1973**, *12*, 310.

143. For some examples, see: (a) Pal, S. K.; Bag, P.; Sarkar, A.; Chi, X.; Itkis, M. E.; Tham, F. S.; Donnadieu, B. and Haddon, R. C. *J. Am. Chem. Soc*. **2010**, *132*, 17258. (b) Haddon, R. C.; Sarkar, A.; Pal, S. K.; Chi, X.; Itkis, M. E. and Tham, F. S. *J. Am. Chem. Soc*. **2008**, *130*, 13683. (c) Pal, S. K.; Itkis, M. E.; Tham, F. S.; Reed, R. W.; Oakley, R. T.; Donnadieu, B. and Haddon, R. C. *J. Am. Chem. Soc.* **2007**, *129*, 7163. (d) Mandal, S. K; Samanta, S.; Itkis, M. E.; Jensen, D. W.; Reed, R. W.; Oakley, R. T.; Tham, F. S.; Donnadieu, B. and Haddon, R. C. *J. Am. Chem. Soc*. **2006**, *128*, 1982. (e) Mandal, S. K.; Itkis, M. E.; Chi, X.; Samanta, S.; Lidsky, D.; Reed, R. W.; Oakley, R. T.; Tham, F. S. and Haddon, R. C. *J. Am. Chem. Soc*. **2005**, *127*, 8185. (f) Pal, S. K.; Itkis M. E.; Tham, F. S.; Reed, R. W.; Oakley, R. T. and Haddon, R. C. *Science* **2005**, *309*, 281. (g) Miller, J. S. *Angew. Chem. Int. Ed*. **2003**, *42*, 27. (h) Chi, X.; Itkis, M. E.; Kirschbaum, K.; Pinkerton, A. A.; Oakley, R. T.; Cordes, A. W. and Haddon, R. C. *J. Am. Chem. Soc*. **2001**, *123*, 4041. (i) Chi, X.; Itkis, M. E.; Patrick, B. O.; Barclay, T. M.; Reed, R. W.; Oakley, R. T.; Cordes, A. W. and Haddon, R. C. *J. Am. Chem. Soc*. **1999**, *121*, 10395.

144. For some examples, see: (a) Ito, A.; Hata, K.; Kawamoto, K.; Hirao, Y.; Tanaka, K.; Shiro, M.; Furukawa, K. and Kato, T. *Chem.-Eur. J*. **2010**, *16*, 10866. (b) Hirao, Y.; Urabe, M.; Ito, A. and Tanaka, K. *Angew. Chem., Int. Ed*. **2007**, *46*, 3300. (c) Ito, A.; Urabe, M. and Tanaka, K. *Angew. Chem., Int. Ed*. **2003**, *42*, 921.

145. Chivers, T.; Eisler, D. J.; Fedorchuk, C.; Schatte, G.; Tuononen, H. M. and Boeré, R. T. *Chem. Commun*. **2005**, 3930.

146. For a review, see: Cordes, A. W.; Haddon, R. C. and Oakley, R. T. *Phosphorus Sulfur Silicon Rel. Elem*. **2004**, *179*, 673.

147. Wood, T. K.; Piers, W. E.; Keay, B. A. and Parvez M. *Chem. Commun*. **2009**, 5147.

148. (a) Baker, R. J.; Farley, R. D.; Jones, C.; Mills, D. P.; Kloth, M. and Murphy, D. M. *Chem.-Eur. J*. **2005**, *11*, 2972. (b) Schoeller, W. W. and Grigoleit, S. *J. Chem. Soc., Dalton Trans*. **2002**, 405. (c) Pott, T.; Jutzi, P.; Kaim, W.; Schoeller, W. W.; Neumann, B.; Stammler, A.; Stammler, H.-G. and Wanner, M. *Organometallics* **2002**, *21*, 3169. (d) Cloke, F. G. N.; Dalby, C. I.; Daff, P. J. and Green, J. C. *J. Chem. Soc., Dalton Trans*. **1991**, 181. (e) Cloke, F. G. N.; Dalby, C. I.; Henderson, M. J.; Hitchcock, P. B.; Kennard, C. H. L.; Lamb, R. N. and Raston, C. L. *J. Chem. Soc., Chem. Commun*. **1990**, 1394.

149. For some recent reviews, see: (a) Holland, P. L. *Acc. Chem. Res*. **2008**, *41*, 905. (b) Cramer, C. J. and Tolman, W. B. *Acc. Chem. Res*. **2007**, *40*, 601. (c) Mindiola, D. J. *Acc. Chem. Res*. **2006**, *39*, 813. (d) Roesky, H. W.; Singh, S.; Jancik, V. and Chandrasekhar, V. *Acc. Chem. Res*. **2004**, *37*, 969. (e) Bourget-Merle, L.; Lappert, M. F. and Severn, J. S. *Chem. Rev*. **2002**, *102*, 3031.

150. (a) Khusniyarov, M. M.; Bill, E.; Weyhermüller, T.; Bothe, E. and Wieghardt, K. *Angew. Chem., Int. Ed.* **2011**, *50*, 1652. (b) Avent, A. G.; Hitchcock, P. B.; Khvostov, A. V.; Lappert, M. F. and Protchenko, A. V. *Dalton Trans.* **2004**, 2272. (c) Eisenstein, O.; Hitchcock, P. B.; Khvostov, A. V.; Lappert, M. F.; Maron, L.; Perrin, L. and Protchenko, A. V. *J. Am. Chem. Soc.* **2003**, *125*, 10790. (d) Avent, A. G.; Khvostov, A. V.; Hitchcock, P. B. and Lappert, M. F. *Chem. Commun*. **2002**, 1410.

151. Kuhn, N.; Fuchs, S.; Maichle-Mössmer, C. E. and Niquet, E. *Z. Anorg. Allg. Chem*. **2000**, *626*, 2248.

152. Dyker, G. and Muth, O. *Eur. J. Org. Chem*. **2004**, 4319.